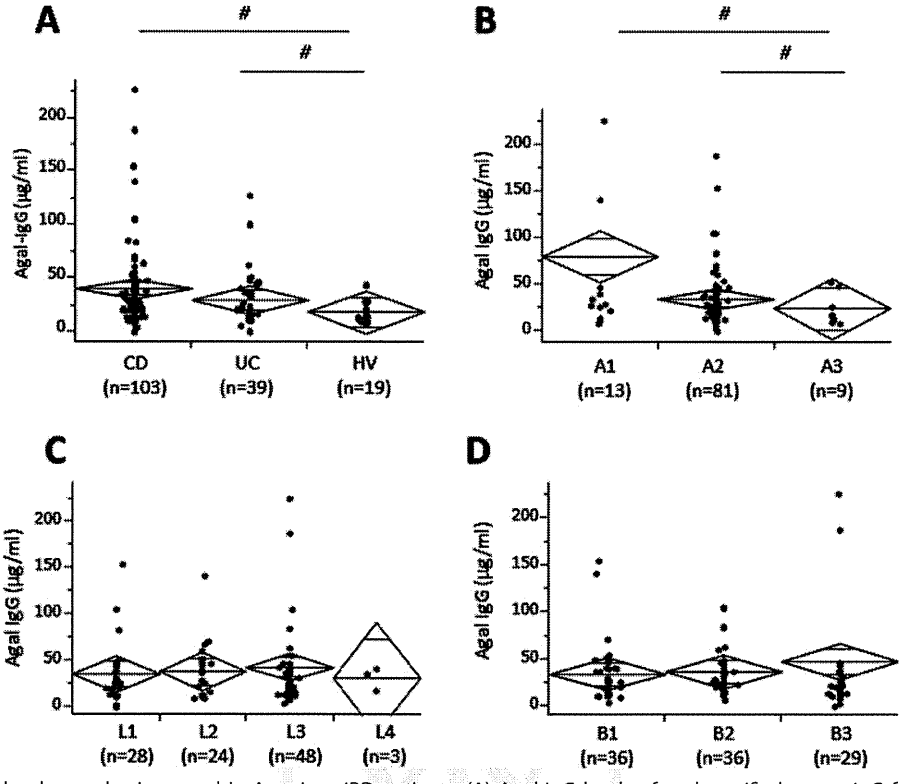

FIGURE 6. Agal-IgG levels are also increased in American IBD patients. (A) Agal-IgG levels of each purified serum IgG from CD, UC, and HV by EIA. (B) Agal-IgG levels and onset age (category A) in CD patients. Agal-IgG levels were significantly higher in patients with category A1 than with A2 or A3. (C,D) Agal-IgG levels and disease location (category L, (B)) and behaviors (category B, (C)) in CD patients.

antibody binding,[10] so lectin-oligosaccharide complexes easily dissociate during the EIA procedure. Second, the recognition of an oligosaccharide by a lectin is not always specific for a single structure. Third, oligosaccharides are sometimes sterically encumbered by the surrounding protein so that lectins do not bind to glycoproteins compared to oligosaccharide structures without proteins. To overcome these problems, we adopted a simultaneous detection system by two lectins. We showed that both lectins recognize agalactosyl IgG oligosaccharides, but the binding affinity of each lectin to oligosaccharide might be subtly influenced by the surrounding protein structure.[27] The Agal-IgG EIA may have achieved a high sensitivity because each lectin contributes to bind to agalactosyl IgG. Another reason the dual lectin Agal-IgG EIA may be a sensitive and specific method is that nonspecific binding for each lectin may decrease due to the requirement for reduced concentrations: A higher concentration of a single lectin is necessary to generate a standard curve for agalactosyl IgG.

We previously reported on the significance of agalactosyl fraction of the fucosylated IgG oligosaccharides (G0F/G2F) in patients with IBD. It is interesting that fucosylated G0F/G2F is more specific than nonfucosylated agalatosyl IgG in IBD.[7] Agal-IgG should be consistent with G0F/G2F by HPLC, because Agal-IgG theoretically indicates whole agalactosyl IgG, and because G0F/G2F is a major fraction of IgG oligosaccharides. In contrast, fucosylation of IgG alters biological activity of IgG including antibody-dependent cellular cytotoxicity, which might be due to conformation changes in the IgG Fc portion.[28] In our system ABA and GSL-II can recognize both the oligosaccharide structure and the 3D structure of the IgG Fc portion, whereas the HPLC system purely analyzes the oligosaccharide structure of IgG. The sensitivity and specificity of Agal-IgG for diagnosis of CD might, therefore, be slightly different from our previous study. However, Agal-IgG could be a marker for disease activity of CD and the combination of Agal-IgG and ASCA is a better marker for diagnosing IBD than ASCA alone, as discussed below. Furthermore, certain cases of CD showed dramatic increases in Agal-IgG measured by lectin-EIA, compared to other IBD and autoimmune diseases. Although we started the present study to establish more convenient methods to measure agalactosyl IgG levels than the HPLC system, Agal-IgG by lectin-EIA can possibly help elucidate the novel pathogenesis of CD. Further studies from both clinical and

J_ID: IBD Customer A_ID: 11-0810.R1 Cadmus Art: IBD22993 Date: 17-April-12 Stage: Page: 10

basic approaches will be required for CD patients showing extremely high Agal-IgG levels.

Here we demonstrated that Agal-IgG is a useful diagnostic marker in combination with ASCA. ASCA is one of the most well-established serologic markers for diagnosing CD,[4] but ASCA alone does not possess enough power to diagnose CD with sufficient sensitivity or specificity. Therefore, ASCA has been combined with other markers, such as peripheral antineutrophil cytoplasmic antibody[5] or anti-outer membrane porin protein C, and anti-CBir1 flagellin.[6] In the present study, Agal-IgG itself showed almost the same sensitivity and specificity as ASCA for the discrimination of CD and HV or CD and UC; however, Agal-IgG was not strongly correlated with ASCA. The combination of Agal-IgG and ASCA could augment the specificity as a diagnostic marker partly because Agal-IgG might identify different subgroups of patients within CD than ASCA. Further investigation is necessary to assess whether the combination of Agal-IgG and ASCA is a better marker for diagnosing IBD than Agal-IgG or ASCA alone. Moreover, we showed that Agal-IgG may have higher predictability for response to infliximab compared with CRP (Fig. 4E,F). Agal-IgG can reflect different inflammatory conditions from CRP, because Agal-IgG is not increased in patients with acute intestinal inflammation (Fig. 3C), and because IgG has a long serum half-life of 3 weeks, whereas that of CRP is 4–6 hours. The decrease of Agal-IgG in 6 weeks of infliximab treatment may be, therefore, a novel marker for sustained response. If confirmed in larger prospective analyses, this finding could have important clinical implications.

In a validation study, we showed that Agal-IgG levels were also significantly increased in a non-Asian, U.S. cohort of IBD patients, especially in early onset (category A1/A2) CD patients. A previous report showed that disease location and clinical course are severer in patients whose onset is younger, and that the A3 group had a lower incidence of fistulas and fewer requirements for immunomodulators and corticosteroids.[29] Higher levels of Agal-IgG in category A1/A2 patients may therefore reflect disease severity in younger-onset patients. Although the mechanism has not been clarified, Agal-IgG can be useful especially for screening pediatric patients for whom invasive studies are hard to perform. Although clinical manifestations appear to be similar in all geographies, ethnic differences in genetic associations have been reported. For instance, mutations in the leucine-rich repeats (LRRs) of nucleotide-binding oligomerization domain containing 2 (NOD2) are associated with an increased risk for CD in many Caucasian populations,[30–32] but not in Japanese patients.[33] Therefore, it is of interest that increases in Agal-IgG levels are observed in Japanese and American IBD patients because of the clinical implications as a diagnostic marker, but also as a reason to explore IgG glycosylation as a global defect in the pathogenesis of IBD.

An increase in serum agalactosyl IgG is also reported in other diseases such as RA,[34] SLE,[35] and tuberculosis.[36] In the present study we showed that Agal-IgG levels were significantly increased in patients with RA and SLE. Agal-IgG might be an effective serological marker for other immunological disorders such as SLE and RA. In addition, Agal-IgG levels in patients with CD are significantly higher than those with SLE and relatively higher than those with RA. Agalactosyl IgG seems to have different functions in each disease, because our recent studies show that the levels of anti-agalactosyl IgG antibodies are increased in the sera of RA[37] but not IBD patients.[7] Moreover, the lectin-complement pathway is activated through agalactosyl IgG in RA[38] but not IBD.[8] Therefore, the availability of an Agal-IgG lectin-EIA will help in translational studies to elucidate mechanisms through which agalactosyl IgG contributes to pathogenesis in different diseases.

In conclusion, the Agal-IgG lectin-EIA system for agalactosyl IgG may represent a novel biomarker assay for IBD. The presence of Agal-IgG in numerous autoinflammatory diseases has potential significance as a diagnostic marker that may fill important clinical needs, and may provide further information about pathogenesis.

ACKNOWLEDGMENTS

We thank Drs. Harumasa Yoshihara and Riichiro Nezu at Osaka Rosai Hospital and Dr. Satoshi Serada at Laboratory for Immune Signal, National Institute of Biomedical Innovation for providing serum samples.

REFERENCES

1. Behm BW, Bickston SJ. Tumor necrosis factor-alpha antibody for maintenance of remission in Crohn's disease. *Cochrane Database Syst Rev.* 2008:CD006893.
2. Prefontaine E, Macdonald JK, Sutherland LR. Azathioprine or 6-mercaptopurine for induction of remission in Crohn's disease. *Cochrane Database Syst Rev.* 2010:CD000545.
3. Cannom RR, Kaiser AM, Ault GT, et al. Inflammatory bowel disease in the United States from 1998 to 2005: has infliximab affected surgical rates? *Am Surg.* 2009;75:976–980.
4. Main J, McKenzie H, Yeaman GR, et al. Antibody to Saccharomyces cerevisiae (bakers' yeast) in Crohn's disease. *BMJ.* 1988;297:1105–1106.
5. Quinton JF, Sendid B, Reumaux D, et al. Anti-Saccharomyces cerevisiae mannan antibodies combined with antineutrophil cytoplasmic autoantibodies in inflammatory bowel disease: prevalence and diagnostic role. *Gut.* 1998;42:788–791.
6. Benor S, Russell GH, Silver M, et al. Shortcomings of the inflammatory bowel disease Serology 7 panel. *Pediatrics.* 2010;125:1230–1236.
7. Shinzaki S, Iijima H, Nakagawa T, et al. IgG oligosaccharide alterations are a novel diagnostic marker for disease activity and the clinical course of inflammatory bowel disease. *Am J Gastroenterol.* 2008;103:1173–1181.
8. Nakajima S, Iijima H, Shinzaki S, et al. Functional analysis of agalactosyl IgG in inflammatory bowel disease patients. *Inflamm Bowel Dis.* 2011;17:927–936.
9. Matsumoto H, Shinzaki S, Narisada M, et al. Clinical application of a lectin-antibody ELISA to measure fucosylated haptoglobin in sera of patients with pancreatic cancer. *Clin Chem Lab Med.* 2010;48:505–512.

ID: ananda | Black Lining: [ON] | Time: 19:30 | Path: N:/3b2/IBD#/Vol00000/120126/APPFile/JW-IBD#120126

10. Hirabayashi J. Oligosaccharide microarrays for glycomics. *Trends Biotechnol.* 2003;21:141–143; discussion 143.
11. Lennard-Jones J. Classification of inflammatory bowel disease. *Scand J Gastroenterol Suppl.* 1989;170:2–6; discussion 16–19.
12. Podolsky D. Inflammatory bowel disease (1). *N Engl J Med.* 1991; 325:928–937.
13. Podolsky D. Inflammatory bowel disease (2). *N Engl J Med.* 1991; 325:1008–1016.
14. Satsangi J, Silverberg MS, Vermeire S, et al. The Montreal classification of inflammatory bowel disease: controversies, consensus, and implications. *Gut.* 2006;55:749–753.
15. Best W, Becktel J, Singleton J, et al. Development of a Crohn's disease activity index. National Cooperative Crohn's Disease Study. *Gastroenterology.* 1976;70:439–444.
16. Rachmilewitz D. Coated mesalazine (5-aminosalicylic acid) versus sulphasalazine in the treatment of active ulcerative colitis: a randomised trial. *BMJ.* 1989;298:82–86.
17. Hanauer SB, Feagan BG, Lichtenstein GR, et al. Maintenance infliximab for Crohn's disease: the ACCENT I randomised trial. *Lancet.* 2002;359:1541–1549.
18. Kuno A, Uchiyama N, Koseki-Kuno S, et al. Evanescent-field fluorescence-assisted lectin microarray: a new strategy for glycan profiling. *Nat Methods.* 2005;2:851–856.
19. Yamada Y, Hosoda T, Yoshizawa M, et al. Development and evaluation of the lectin-enzyme immune assay kit for detection of anti-agalactosyl IgG antibodies. *Clin Rep.* 1997;31:81–101.
20. Beck JR, Shultz EK. The use of relative operating characteristic (ROC) curves in test performance evaluation. *Arch Pathol Lab Med.* 1986;110:13–20.
21. Zweig MH, Campbell G. Receiver-operating characteristic (ROC) plots: a fundamental evaluation tool in clinical medicine. *Clin Chem.* 1993;39:561–577.
22. Nakamura-Tsuruta S, Kominami J, Kamei M, et al. Comparative analysis by frontal affinity chromatography of oligosaccharide specificity of GlcNAc-binding lectins, Griffonia simplicifolia lectin-II (GSL-II) and Boletopsis leucomelas lectin (BLL). *J Biochem.* 2006;140: 285–291.
23. Nakamura-Tsuruta S, Kominami J, Kuno A, et al. Evidence that Agaricus bisporus agglutinin (ABA) has dual sugar-binding specificity. *Biochem Biophys Res Commun.* 2006;347:215–220.
24. Kornfeld R, Ferris C. Interaction of immunoglobulin glycopeptides with concanavalin A. *J Biol Chem.* 1975;250:2614–2619.
25. Presant CA, Kornfeld S. Characterization of the cell surface receptor for the Agaricus bisporus hemagglutinin. *J Biol Chem.* 1972;247:6937–6945.
26. Chatterjee BP, Ahmed H, Uhlenbruck G, et al. Jackfruit (Artocarpus integrifolia) and the Agaricus mushroom lectin fit also to the so-called peanut receptor. *Behring Inst Mitt.* 1985;148–158.
27. Paulson JC, Blixt O, Collins BE. Sweet spots in functional glycomics. *Nat Chem Biol.* 2006;2:238–248.
28. Huhn C, Selman MH, Ruhaak LR, et al. IgG glycosylation analysis. *Proteomics.* 2009;9:882–913.
29. Magro F, Portela F, Lago P, et al. Crohn's disease in a southern European country: Montreal classification and clinical activity. *Inflamm Bowel Dis.* 2009;15:1343–1350.
30. Hampe J, Cuthbert A, Croucher PJ, et al. Association between insertion mutation in NOD2 gene and Crohn's disease in German and British populations. *Lancet.* 2001;357:1925–1928.
31. Hugot JP, Chamaillard M, Zouali H, et al. Association of NOD2 leucine-rich repeat variants with susceptibility to Crohn's disease. *Nature.* 2001;411:599–603.
32. Ogura Y, Bonen DK, Inohara N, et al. A frameshift mutation in NOD2 associated with susceptibility to Crohn's disease. *Nature.* 2001; 411:603–606.
33. Yamazaki K, Takazoe M, Tanaka T, et al. Absence of mutation in the NOD2/CARD15 gene among 483 Japanese patients with Crohn's disease. *J Hum Genet.* 2002;47:469–472.
34. Parekh RB, Dwek RA, Sutton BJ, et al. Association of rheumatoid arthritis and primary osteoarthritis with changes in the glycosylation pattern of total serum IgG. *Nature.* 1985;316:452–457.
35. Tomana M, Schrohenloher RE, Koopman WJ, et al. Abnormal glycosylation of serum IgG from patients with chronic inflammatory diseases. *Arthritis Rheum.* 1988;31:333–338.
36. Parekh R, Isenberg D, Rook G, et al. A comparative analysis of disease-associated changes in the galactosylation of serum IgG. *J Autoimmun.* 1989;2:101–114.
37. Das H, Atsumi T, Fukushima Y, et al. Diagnostic value of antiagalactosyl IgG antibodies in rheumatoid arthritis. *Clin Rheumatol.* 2004;23:218–222.
38. Malhotra R, Wormald MR, Rudd PM, et al. Glycosylation changes of IgG associated with rheumatoid arthritis can activate complement via the mannose-binding protein. *Nat Med.* 1995;1:237–243.

IJC
International Journal of Cancer

$CD34^+/CD38^-$ acute myelogenous leukemia cells aberrantly express CD82 which regulates adhesion and survival of leukemia stem cells

Chie Nishioka[1,2], Takayuki Ikezoe[3], Mutsuo Furihata[4], Jing Yang[3], Satoshi Serada[5], Tetsuji Naka[5], Atsuya Nobumoto[6], Sayo Kataoka[7], Masayuki Tsuda[6], Keiko Udaka[1] and Akihito Yokoyama[3]

[1] Department of Immunology, Kochi Medical School, Kochi University, Nankoku, Kochi, Japan
[2] Japanese Society for the Promotion of Science (JSPS), Chiyoda-ku, Tokyo, Japan
[3] Hematology and Respiratory Medicine, Kochi Medical School, Kochi University, Nankoku, Kochi, Japan
[4] Tumor Pathology, Kochi Medical School, Kochi University, Nankoku, Kochi, Japan
[5] Laboratory for immune Signal, National Institute of Biomedical Innovation, Ibaraki, Osaka
[6] The Facility for Animal Research, Kochi Medical School, Kochi University, Nankoku, Kochi, Japan
[7] Medical Research Center, Kochi Medical School, Kochi University, Nankoku, Kochi, Japan

To identify molecular targets in leukemia stem cells (LSCs), this study compared the protein expression profile of freshly isolated $CD34^+/CD38^-$ cells with that of $CD34^+/CD38^+$ counterparts from individuals with acute myelogenous leukemia (n = 2, AML) using isobaric tags for relative and absolute quantitation (iTRAQ). A total of 98 proteins were overexpressed, while six proteins were underexpressed in $CD34^+/CD38^-$ AML cells compared with their $CD34^+/CD38^+$ counterparts. Proteins overexpressed in $CD34^+/CD38^-$ AML cells included a number of proteins involved in DNA repair, cell cycle arrest, gland differentiation, antiapoptosis, adhesion, and drug resistance. Aberrant expression of CD82, a family of adhesion molecules, in $CD34^+/CD38^-$ AML cells was noted in additional clinical samples (n = 12) by flow cytometry. Importantly, down-regulation of CD82 in $CD34^+/CD38^-$ AML cells by a short hairpin RNA (shRNA) inhibited adhesion to fibronectin *via* up-regulation of matrix metalloproteinases 9 (MMP9) and colony forming ability of these cells as assessed by transwell assay, real-time RT-PCR, and colony forming assay, respectively. Moreover, we found that down-regulation of CD82 in $CD34^+/CD38^-$ AML cells by an shRNA significantly impaired engraftment of these cells in severely immunocompromised mice. Taken together, aberrant expression of CD82 might play a role in adhesion of LSCs to bone marrow microenvironment and survival of LSCs. CD82 could be an attractive molecular target to eradicate LSCs.

Cancer Cell Biology

Key words: AML, leukemia stem cells, bone marrow microenvironment, CD82, MMP9
Additional Supporting Information may be found in the online version of this article.
*Takayuki Ikezoe contributed to the concept and design, interpreted and analyzed the data and wrote an article. Chie Nishioka performed all experiments and wrote an article. Mutsuo Furihata, Jing Yang, Satoshi Serada, and Tetsuji Naka, Sayo Kataoka and Atsuya Nobumoto performed the experiments. Akihito Yokoyama and Keiko Udaka provided important intellectual content
Grant sponsors: The Kochi University President's Discretionary Grant, Setsuro Fujii Memorial, The Osaka Foundation for Promotion of Fundamental Medical Research, Certificate of Kochi Shin-kin/Anshin-tomo-no-kai Prize and Japan Society for the Promotion of Science
DOI: 10.1002/ijc.27904
History: Received 15 Mar 2012; Accepted 25 Sep 2012; Online 11 Oct 2012
Correspondence to: Takayuki Ikezoe, Department of Hematology and Respiratory Medicine, Kochi University, Oko-cho, Nankoku, Kochi 783-8505, Japan, Tel.: 81-88-880-2345, Fax: 81-88-880-2348, E-mail: ikezoet@kochi-u.ac.jp

Acute myelogenous leukemia (AML) is characterized by a cellular hierarchy, and is initiated and maintained by a subset of self-renewing leukemia stem cells (LSCs).[1] To produce cure in individuals with AML, development of a novel treatment strategy targeting LSCs is urgently required. LSCs share some antigenic features with normal hematopoietic stem cells (HSCs). For example, both LSCs and HSCs express CD34 but not CD38. However, LSCs can be phenotypically distinguished from HSCs by several disparate markers, including $CD117^-$ and $CD123^+$.[1–3] LSCs exist in a quiescent state and are capable of self-renewal and differentiation, and are able to perpetuate leukemic cell growth in long-term culture assays and in the murine nonobese diabetic/severe combined immunodeficiency (NOD/SCID) model system.[1–4] $CD34^+/CD38^-$ AML cells were shown to fulfill the criteria for LSCs *in vivo*.[5,6] Although, recent studies employed more severely immunocompromised mice found that even $CD34^-$ or $CD38^+$ AML cells in some cases were able to reconstitute AML.[7,8]

The regulation of stem cell self-renewal and differentiation requires a specific microenvironment of surrounding cells known as the stem cell niche. The concept of the stem cell niche was first proposed for the human hematopoietic system in the 1970s.[9] The HSC niche in mouse bone marrow (BM) is

What's new?
Acute myelogenous leukemia (AML) is maintained by a subset of self-renewing leukemia stem cells (LSCs). Thus, to effectively treat AML, treatments targeting LSCs are needed. AML cells expressing CD34 but not CD38 (CD34+/CD38-) contain abundant LSCs and were found in this study to express a greater amount of CD82 than CD34+/CD38+ AML cells. CD82 was further found to regulate the survival of CD34+/CD38- AML cells and their adhesion to the bone marrow microenvironment, suggesting that this glycoprotein could be an attractive target for LSC eradication.

composed of an endosteal lining of stromal cells, extracellular matrix proteins, and osteoblasts.[10–12] Specific adherens junction molecules such as N-cadherin mediate adhesion between HSCs and niche cells in the adult hematopoietic system.[11]

Recent work has shown that interaction between CXCR4 on leukemic cells and its ligand stromal cell-derived factor-1 (SDF-1) in the niche is necessary for proper homing and *in vivo* growth of leukemic cells.[13] Moreover, interaction between LSCs and the niche mediated by adhesion molecule CD44 is required for maintenance of LSCs behavior.[14] CD44 mediates adhesive cell-cell and cell-extracellular matrix interactions by binding its main ligand, hyaluronan, a glycosaminoglycan that is highly concentrated in the endosteal region.[14,15] All together, adhesion molecules play an important role in maintaining the characteristics of LSCs.

CD82/KAI-1, a member of the tetraspanin superfamily, was originally identified as an accessory molecule in T-cell activation.[16] The most well-characterized function of CD82 in nonimmune cells is integrin-mediated cell adhesion to extracellular matrix.[17] Forced expression of CD82 up-regulated tissue inhibitors of metalloproteinase 1 (TIMP1) and inactivated matrix metalloproteinases 9 (MMP9) in the H1299 human lung carcinoma cells, resulting in suppression of tumor invasion and metastasis.[18] Cell adhesion to collagen I, which is one of the major proteins in the bone marrow (BM) niche, is mostly mediated by three integrin receptors $\alpha1\beta1$, $\alpha2\beta1$, and $\alpha11\beta1$ expressed on cell surface of mesenchymal stem cells.[19] Integrin may associate with CD82 in $CD34^+/CD38^-$ AML cells to promote adhesion to the endosteal niche. However, the roles of CD82 in hematopoietic cells remain to be elucidated.

In this study, we analyzed the protein expression profile of freshly isolated $CD34^+/CD38^-$ AML cells from individuals with AML and compared it with the expression profile of their $CD34^+/CD38^+$ counterparts using isobaric tags for relative and absolute quantitation (iTRAQ) and found the aberrant expression of CD82 in $CD34^+/CD38^-$ AML cells. This study also explored the function of CD82 in $CD34^+/CD38^-$ AML cells *in vitro* as well as *in vivo* by utilizing NOD.Cg-*Rag1*^{tm1Mom} *Il2rg*^{tm1Wjl}/SzJ mice.

Material and Methods

Sample collection and isolation of $CD34^+/CD38^-$ AML cells and their $CD34^+/CD38^+$ counterparts

Leukemia cells were freshly isolated from AML patients (n = 18) with World Health Organization (WHO) classification system subtype minimally differentiated AML (case 6), AML without maturation (cases 1 and 10), AML with maturation (cases 2, 7, and 12), acute myelomonocytic leukemia (cases 4, 14, and 15), AML with myelodysplasia changes (cases 3, 5, 8, 9,16, 17, and 18), and therapy-related AML (cases 11 and 13) after obtaining informed consent with Kochi University Institutional Review Board approval (Supporting Information Table S1). The informed consent was obtained in accordance with the Declaration of Helsinki. $CD34^+/CD38^-$ AML cells and $CD34^+/CD38^+$ counterparts were purified by magnetic cell sorting utilizing a CD34 MultiSort kit and a CD38 MicroBead kit (Miltenyi Biotec GmbH, Germany), as previously described (Supporting Information Fig. S1*a*).[20]

Cells

Chronic eosinophilic leukemia (CEL) EOL-1 cells were obtained from RIKEN BRC Cell Bank (Tsukuba, Japan). Imatinib-resistant EOL-1R cell line was established by culturing with increasing concentrations of imatinib (from 1 to 100 nM) for 6 months.[21] Most of EOL-1R cells expressed CD34 ($92 \pm 9\%$) on their cell surface. On the other hand, CD34 was rarely detectable on cell surface of parental EOL-1 cells ($0.1 \pm 0.1\%$) (figure not shown).

Isolation and culture of primary mesenchymal stromal cells (MSCs)

MSCs were isolated from a BM of healthy donors. BM cells were subjected to centrifugation over a Ficoll-Hypaque gradient to separate mononuclear cells. These cells were resuspended in α-minimal essential medium (Gibco BRL, Rockville, MD) containing 20% fetal bovine serum (FBS) and plated at an initial density of 10^6 cells.[22]

Protein extraction

Proteins were extracted using the complete mammalian proteome kit (539779, Calbiochem, Darmstadt, Germany), according to the manufacturer's instructions.

iTRAQ labeling of peptides

Each protein sample (100 μg) was digested with trypsin and labeled with iTRAQ reagents (Applied Biosystems, Framingham, MA) according to the manufacturer's instructions. Briefly, the proteins extracted from $CD34^+/CD38^-$ AML cells were labeled with iTRAQ reagents 114 (case 1) or 116 (case 2), and proteins extracted from $CD34^+/CD38^+$ counterparts

Table 1. PCR primers

Gene	Direction	Primer
MMP9	Forward	5′-CTCGAACTTTGACAGCGACA-3′
	Reverse	5′-GCCATTCACGTCGTCCTTAT-3′
MMP2	Forward	5′-ACCCAGATGTGGCCAACTAC-3′
	Reverse	5′-TCATGATGTCTGCCTCTCCA-3′
18S	Forward	5′-AAACGGCTACCACATCCAAG-3′
	Reverse	5′-CCTCCAATGGATCCTCGTTA-3′

were labeled with iTRAQ reagents 115 (case 1) or 117 (case 2). Labeled peptide samples were mixed and fractionated as described previously.[23]

Mass spectrometric analysis

NanoLC-MS/MS analyses were performed on an LTQ-Orbitrap XL (Thermo Fisher Scientific, Waltham, MA) equipped with a nano-ESI source and coupled to a Paradigm MG2 pump (Michrom Bioresources, Auburn, CA) and autosampler (HTC PAL, CTC Analytics, Zwingen, Switzerland).[23]

iTRAQ data analysis

Protein identification and quantitation for iTRAQ analysis was carried out using SEQUEST (Bioworks version 3.3.1, Thermo Fisher Scientific) searching against the International Protein Index (IPI) human protein database (version 3.26).[23] Relative protein abundances were determined by comparing the ratio of iTRAQ reporter ion intensities in the MS/MS scan.[23]

Quantitation of CD82-expressing cells using flow cytometry (FACS)

Leukemic peripheral blood (PB) ($n = 3$) and BM ($n = 9$) cells were collected from 12 AML patients (case numbers 1–12) after obtaining informed consent. Leukemic cells were stained with a fluorescein isothiocyanate (FITC)-conjugated monoclonal antibody (mAb) against CD34 (Beckman coulter, CA), a phycoerythrin (PE)-conjugated mAb against CD82 (Abcam, Cambridge, UK), and a PE Cy5-conjugated mAb against CD38 (BioLegend, San Jose, CA). Cells were stained for 30 min on ice. Isotypo-matched immunoglobulins were used as controls. Cells were then analyzed using flow cytometry (FACS Calibur, Becton Dickinson, San Jose, CA) following data analysis by FlowJo software (TreeStar, San Carlos, CA).

RNA isolation and real-time reverse transcription-polymerase chain reaction (RT-PCR)

RNA isolation and cDNA preparation were performed as described previously.[24] Real-time RT-PCR was carried out by using Power SYBR Green PCR Master Mix (Applied Biosystems, Warrington, UK) as described previously.[24] Primers for PCR are shown in Table 1.

Small interfering RNA

Control small interfering (si) RNA and an siRNA against CD82 were purchased from Santa Cruz Biotechnology and Sigma (Deisenhofen, Germany), respectively.

Transfections

EOL-1 and EOL-1R cells were transiently transfected with either control or CD82 siRNA (300 nM) using an Amaxa Nucleofector II electroporator (Wako Pure Chemical Industries, Ltd., Osaka, Japan) with a Nucleofector Kit V (program U-001) as previously described.[25] The preliminary experiments using the green fluorescence protein-expressing vector found that efficacy of transfection with this program was approximately 70% with nearly 70% cell viability, as measured by FACS and Annexin V/PI staining, respectively (figure not shown).

CD82 shRNA lentiviral vector, production and infection

The short hairpin (sh) RNA sequence used to target human CD82 corresponded to the following sequence on the human CD82 transcript variant 2, NCB I accession number NM_001024844. Lentiviral shRNA particles were produced using the viral power packaging system (Invitrogen, CA) with the 293FT packaging cell line (Invitrogen), and lentiviral CD82 shRNA particles (>10^8 titer unit (TU)/ml) were prepared using ultracentrifugation. 5×10^4 $CD34^+/CD38^-$ AML cells were seeded in 24-well plates in 500 μl of Iscove's modified Dulbecco's medium (IMDM) (Invitrogen) containing 10% heat inactivated fetal bovine serum (FBS). After overnight incubation, 5×10^5 TU lentiviral CD82 shRNA particles and polybrene (10 μg/ml) were added per well with serum free medium containing IMDM. After overnight, 1 ml of full media supplemented with FBS, 2-mercaptoethanol, stem cell factor, granulocyte-macrophage colony-stimulating factor (GM-CSF), granulocyte-colony-stimulating factor (G-CSF), IL-3, and erythropoietin (EPO) was added and incubated for 7 days. The control and CD82 shRNA lentiviral vectors co-expressed green fluorescence protein (GFP). Quantification of GFP-positive cells using FACS analysis indicated that the lentiviral transduction efficiency was nearly 70% (Supporting Information Fig. S1*b*). GFP-positive cells were sorted using JSAN (Bay bioscience Co., Ltd., Kobe, Japan).

CD82 lentiviral vector

CD82 cDNA was purchased from Mammalian gene collection (BC000726) and was used as the template for PCR. PCR products were cloned into pLenti6.3/V5-TOPO vector (Invitrogen). CD82-transfected lentiviral particles were produced using the viral power packaging system (Invitrogen) with the 293FT packaging cell line (Invitrogen). The pLenti6.3/V5-TOPO vector was designed to co-express V5 epitope; 5×10^4 $CD34^+/CD38^+$ AML cells were seeded in 24-well plates in 500 μl of IMDM (Invitrogen) containing 10% FBS. After overnight incubation, 5×10^5 TU lentiviral CD82-transfected

lentiviral particles and polybrene (10 μg/ml) were added per well. After overnight, supernatant was removed and 1 ml of full media was added and incubated for 7 days. FACS analysis utilizing an anti-V5 antibody (Invitrogen, R960-25) indicated that the efficiency of transduction into $CD34^+/CD38^+$ AML cells was nearly 80% (Supporting Information Fig. S1*b*).

Migration assays

Freshly isolated either $CD34^+/CD38^-$ (5×10^5 cells) or $CD34^+/CD38^+$ AML cells (1×10^5 cells) were transduced by either CD82 shRNA or CD82 cDNA, respectively, and then seeded in the upper inserts with 3 μm pores coated by fibronectin (Cat. No. 354543, Becton Dickinson Biosciences, Bedford, MA) and mesenchymal stromal cells (MSCs) established from healthy donors, while the lower wells were filled with Iscove's Modified Dulbecco's Medium (IMDM) containing 10% heat inactivated FBS. Similarly, EOL-1 and EOL-1R cells were transiently transfected with either control or CD82 siRNA. After 48 hr, these cells (5×10^5 cells in 100 μl RPMI-1640) were seeded in the upper biocoat cell culture inserts coated by fibronectin, and the lower well was filled to the top with RPMI-1640 containing 10% heat inactivated FBS as a chemoattractant. After incubation for 48 hr, the supernatant was discarded and the cells that had adhered to the fibronectin were gently washed in phosphate-buffered saline (PBS). Cells were then fixed for 1 hr in 4% paraformaldehyde, washed twice in PBS, stained with 4'6-diamidino-2-phenylindole (DAPI), and counted under a microscope (OLYMPUS FV1000-D). The cells that had passed through the membrane filter were collected and the number of viable cells was counted under light microscope after staining with trypan blue.

Gelatin zymography

The culture supernatant as well as whole cell proteins of EOL-1 and EOL-1R cells were harvested. Gelatinolytic activities were carried out by utilizing a gelatin-zymography kit (Primarycell, Hokkaido, Japan). Each lane was loaded with 30 μg of whole protein lysates or 20 μl of supernatant.

Colony forming assay

The colony-forming assay was performed with methylcellulose medium H4034 (StemCell Technologies, Vancouver, BC, Canada), as previously described.[20]

Bone marrow transplantation and engraftment assay

NOD.Cg-*Rag1*^{tm1Mom} *Il2rg*^{tm1Wjl}/SzJ mice (Stock number: 007799) were purchased from the Jackson Laboratory for experimental animals (Bar Harbor)[26] and bred in a pathogen-free environment in accordance with the guidelines of the Kochi University School of Medicine. The 6-week-old mice were utilized for experiments. $CD34^+/CD38^-$ AML cells (1×10^4 cells) transfected with either scrambled control or CD82 shRNA were injected to each mouse intravenously *via* the tail vein. At 9 weeks after transplantation, mice were euthanized and BM were removed. BM cells were flushed from the femurs using 25-gauge needles (Becton Dickinson Biosciences) and then fixed in formalin. The human cell engraftment was analyzed by using flow cytometry after staining of spleen cells with human CD45 PE Cy5-conjugated mAb (Dako, Glostrup, Denmark) and human CD33 PE-conjugated mAb (Becton Dickinson Biosciences).

Single cell RT-PCR

A single $CD34^+/CD38^-$ AML cell was isolated by BD FACS AriaII (Becton Dickinson Biosciences) and subjected to RT-PCR by AmpliSpeed slide cycler (Beckman Coulter, Munich, Germany) and ABI StepOnePlus (Applied Biosystems) to measure the levels of CD82 and MMP9.

Immunohistochemistry of CD82 in BM sections

Immunohistochemical staining of CD82 was performed with a Ventana DISCOVERYTM autostainer system (Ventana Japan, Osaka, Japan) as previously described.[25] The anti-CD82 antibody (Santa Cruz Biotechnology, Santa Cruz, CA) was used.

Cell cycle analysis by flow cytometry (FACS)

Cell cycle distribution of $CD34^+/CD38^-$ AML cell was measured as previously described after transduction of either scrambled control or CD82 shRNA. Briefly, the cells were stained with Ki-67 (Santa Cruz Biotechnology) and propidium iodide and subjected to FACS.[20]

Homing analysis

The human AML cells isolated from patients were treated with anti-human CD82 (Santa Cruz Biotechnology) or control IgG (eBiosScience, San Diego, CA) antibody on ice for 1 hr. This anti-CD82 antibody worked as a neutralizing antibody (Nishioka *et al.* unpublished data). Cells were washed gently with PBS and were injected to each mouse intravenously *via* the tail vein. At 16 hr after transplantation, mice were euthanized and BMs were removed and analyzed by flow cytometry with anti-human CD45 and CD34 antibodies. We acquired in the range of 1×10^6 to 3×10^6 events per sample.

Statistical analysis

When comparing two groups, Student's *t*-test was used. For demonstration of association, the Pearson's correlation coefficient test was applied. All statistical analyses were carried out using SPSS software (Version 11.03; spss, Tokyo, Japan) and the results were considered to be significant when the p value was <0.05, and highly significant when the p value was <0.01.

Results

Protein expression profiles of $CD34^+/CD38^-$ AML cells and $CD34^+/CD38^+$ counterparts

Four samples (two from $CD34^+/CD38^-$ AML cells lysates and two from $CD34^+/CD38^+$ counterparts lysates, approximately 10 million cells per sample) were trypsinized and

Table 2. Protein expression profiles of $CD34^+/CD38^-$ and $CD34^+/CD38^+$ AML cells

NCBI accession no.	Protein	Average iTRAQ ration (114/115)	Average iTRAQ ration (116/117)	Gene symbol
P27701	Adhesion: CD82 antigen	4.64	3.79	CD82 (KAI1)
Q9H165	Apoptosis: Isoform 1 of B-cell lymphoma/leukemia 11A	5.79	6.38	BCL11A (CTIP1)
P47738	Enzyme: Aldehyde dehydrogenase, mitochondrial precursor	5.22	4.43	ALDH
Q9H0C8	Enzyme: Integrin-linked kinase-associated serine/threonine phosphatase 2C	4.29	10.52	ILKAP
P01903	Immunity: HLA class II histocompatibility antigen, DR alpha chain precursor	6.11	3.87	HLA-DRA

labeled with a specific isobaric iTRAQ reagent. To compensate for extreme sample complexity, each iTRAQ sample was separated into 24 fractions using strong cation-exchange chromatography.[23] A total of 2,537 and 2,506 proteins were identified with >95% confidence for each of the biological replicates. Since iTRAQ internal replicates typically yield high confidence results,[27] differences greater than threefold or less than 0.5-fold are considered significant. We listed the proteins whose expression was greater than 3-fold or less than 0.5-fold in $CD34^+/CD38^-$ AML cells as compared with their $CD34^+/CD38^+$ counterparts in Table 2 and Supporting Information Table 2. Either 481 or 700 proteins were differentially expressed in case 1 and case 2, respectively (Table not shown), and only 104 proteins were overlapped in both cases (Table 2, Supporting Information Table S1).The expression of 98 of these proteins increased, while the expression of six proteins decreased in both cases (Table 2, Supporting Information Table S1). Two of the identified proteins are involved in differentiation, two play a role in the cell cycle, six play a role in adhesion, five are involved in DNA replication and repair, and eight are involved in apoptosis and anti-apoptosis (Table 2, Supporting Information Table S1). In addition, 6 nuclear transcription factors, 17 enzymes involved in drug-resistance, 6 human leukocyte antigens, 18 ribosome nucleoproteins, and 10 histone and histone-binding proteins were differentially expressed between $CD34^+/CD38^-$ AML and $CD34^+/CD38^+$ counterparts (Supporting Information Table S1). Additional differentially expressed proteins are also listed in Supporting Information Table S1. Other studies identified aldehyde dehydrogenase activity (ALDH), B-cell lymphoma/leukemia 11A (BCL11A), ILK, and HLA-DR as highly expressed proteins in leukemia stem cells.[28–31] These proteins were also overexpressed in $CD34^+/CD38^-$ AML cells in the present study (Table 2), indicating an acceptable sensitivity of the current study.

CD82 is overexpressed in $CD34^+/CD38^-$ AML cells

We focused on CD82 because this protein functions as an adhesion molecule that is important to maintain the character of LSCs. We attempted to validate these results in other $CD34^+/CD38^-$ AML cells isolated from patients (11 from BM, 5 from PB, cases 1–14, 17, 18) by FACS. In 15 of 16 cases (94%), the relative expression levels of CD82 were significantly higher in $CD34^+/CD38^-$ AML cells (68 ± 27%) as compared with their $CD34^+/CD38^+$ counterparts (30 ± 19%) ($p < 0.01$, Fig.1*a*, Supporting Information Fig. S2*a*). On the other hand, a mean 35 ± 19% of $CD34^+$ hematopoietic stem/progenitor cells isolated from healthy volunteers ($n = 6$) were positive for CD82 staining (Supporting Information Fig. S2*b*). In addition, we found that imatinib-resistant EOL-1R cells which stayed on a dormant state and possessed the immature character with aberrant expression of CD34 (data not shown) expressed a greater amount of CD82 on their cell surface (96 ± 1%) than parental EOL-1 cells (47 ± 4%) (Fig. 1*a*).

The MMPs enzymatic activity

Aberrant expression of CD82 was associated with inactivation of matrix metalloproteinase 9 (MMP9) in the H1299 human lung carcinoma cells.[14] We therefore examined the relationship between CD82 and MMPs in $CD34^+/CD38^-$ AML cells. Real-time RT-PCR found that the levels of MMP9 were significantly lower in CD82 over-expressed $CD34^+/CD38^-$ AML cells than their $CD34^+/CD38^+$ counterparts ($n = 7$, $p < 0.01$) (Fig. 1*b*). On the other hand, levels of MMP2 in $CD34^+/CD38^-$ AML cells were almost identical to those in $CD34^+/CD38^+$ counterparts (Fig. 1*b*). We also found that the levels of both MMP-9 and -2 were down-regulated in imatinib-resistant EOL-1R cells as compared with parental EOL-1 cells (Fig. 1*b*). To explore a potential link between CD82 and MMPs in leukemia cells, EOL-1R cells were transiently transfected with either scrambled control or CD82 siRNA (Fig. 1*c*), which efficiently decreased levels of CD82 in these cells (from 96 ± 1% to 41 ± 1%, Fig. 1*c*). The MMPs enzymatic activity in these cells was determined by performing gelatin zymography with the culture supernatant as well as whole cell proteins extracted from EOL-1 and EOL-1R cells (Fig. 1*d*). Interestingly, when CD82 was down-regulated in EOL-1R cells by an siRNA, enzymatic activity of MMP9 was dramatically increased (Fig. 1*d*), suggesting that CD82 negatively regulated MMP9. Real-time RT-PCR found that

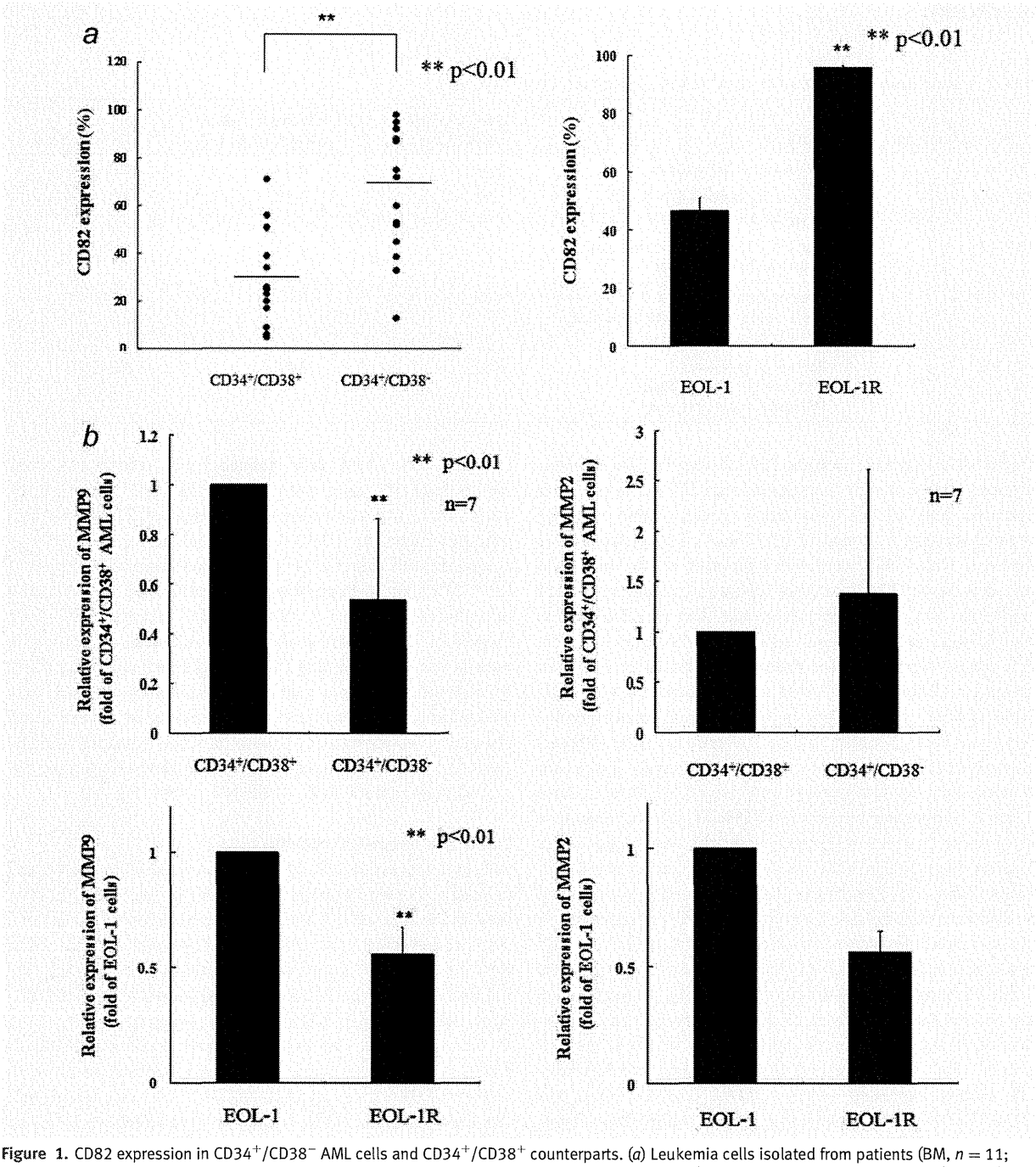

Figure 1. CD82 expression in $CD34^+/CD38^-$ AML cells and $CD34^+/CD38^+$ counterparts. (*a*) Leukemia cells isolated from patients (BM, $n = 11$; PB, $n = 5$) were stained with anti-CD34, -CD38, and -CD82 antibodies. Expression of CD82 in $CD34^+/CD38^-$ AML cells and their $CD34^+/CD38^+$ counterparts was analyzed using FlowJo. Each dot represents expression of CD82 for an individual and the mean value is indicated by the line. EOL-1 or EOL-1R cells were stained with anti-CD82 antibody. Expression of CD82 in EOL-1 or EOL-1R cells was analyzed using FlowJo. Statistical significance was determined by paired *t*-test. $^{**}p < 0.01$, with respect to control. The effect of CD82 on MMPs. Real-time RT-PCR. (*b*) RNA was extracted from EOL-1, EOL-1R, and $CD34^+/CD38^-$ cells and their $CD34^+/CD38^+$ counterparts isolated from AML patients. cDNAs were synthesized and subjected to real-time RT-PCR to measure the levels of MMP9 and MMP2. Results represent the mean ± SD of three experiments performed in triplicate. The statistical significance was assessed by a paired *t*-test. $^{**}p < 0.01$;$^{*}p < 0.05$. FACS. (*c*) EOL-1 cells were transiently transfected with either scrambled control or CD82 siRNA. After 24 hr, cells were subjected to FACS to quantity the proportion of CD82-expressing cells. Gelatin zymography. (*d*) EOL-1 and EOL-1R cells were transfected with either scrambled control or CD82 siRNA. After 48 hr, whole cell lysates and culture supernatant were collected. The enzymatic activity of MMPs was determined by a gelatin-zymography kit, following the manufacturer's instructions. Real-time RT-PCR. (*e*) EOL-1R cells were transfected with either scrambled control or CD82 siRNA. After 24 hr, these cells were collected and mRNAs were extracted. cDNAs were synthesized and subjected to real-time RT-PCR to measure the levels of MMP9 and MMP2. Results represent mean ± SD of duplicate cultures. $^{**}p < 0.01$; $^{*}p < 0.05$. FACS. (*f*) $CD34^+/CD38^-$ AML cells (cases 1, 2, 6, and 14) were transduced with either control or CD82 shRNA. (*h*) $CD34^+/CD38^+$ AML cells (cases 1, 2, 14, and 15) were transduced with either empty vector or CD82-expressing lentiviral particles. These cells were subjected to FACS to quantity the proportion of CD82-expressing cells. Real-time RT-PCR. (*g*) $CD34^+/CD38^-$ (cases 1, 2, and 6) or (i) $CD34^+/CD38^+$ AML cells (cases 1, 2, 14, and 15) transduced with CD82 shRNA or CD82-expressing lentiviral particles were collected and mRNAs were extracted. cDNAs were synthesized and subjected to real-time RT-PCR to measure the levels of MMP9. Each dot represents the levels of MMP9 for an individual experiment and the mean is indicated by the line. $^{**}p < 0.01$; $^{*}p < 0.05$.

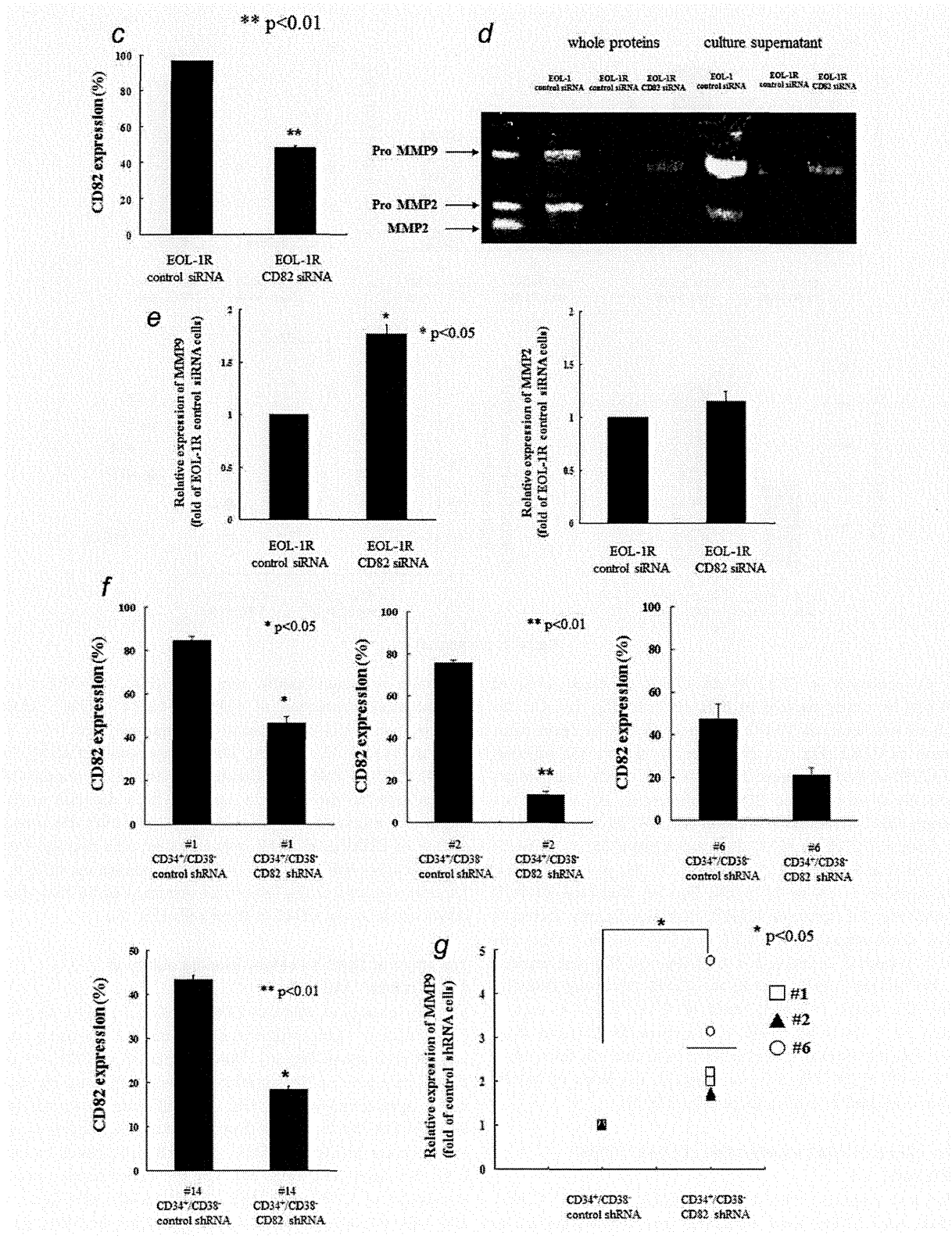

Figure 1. (Continued)

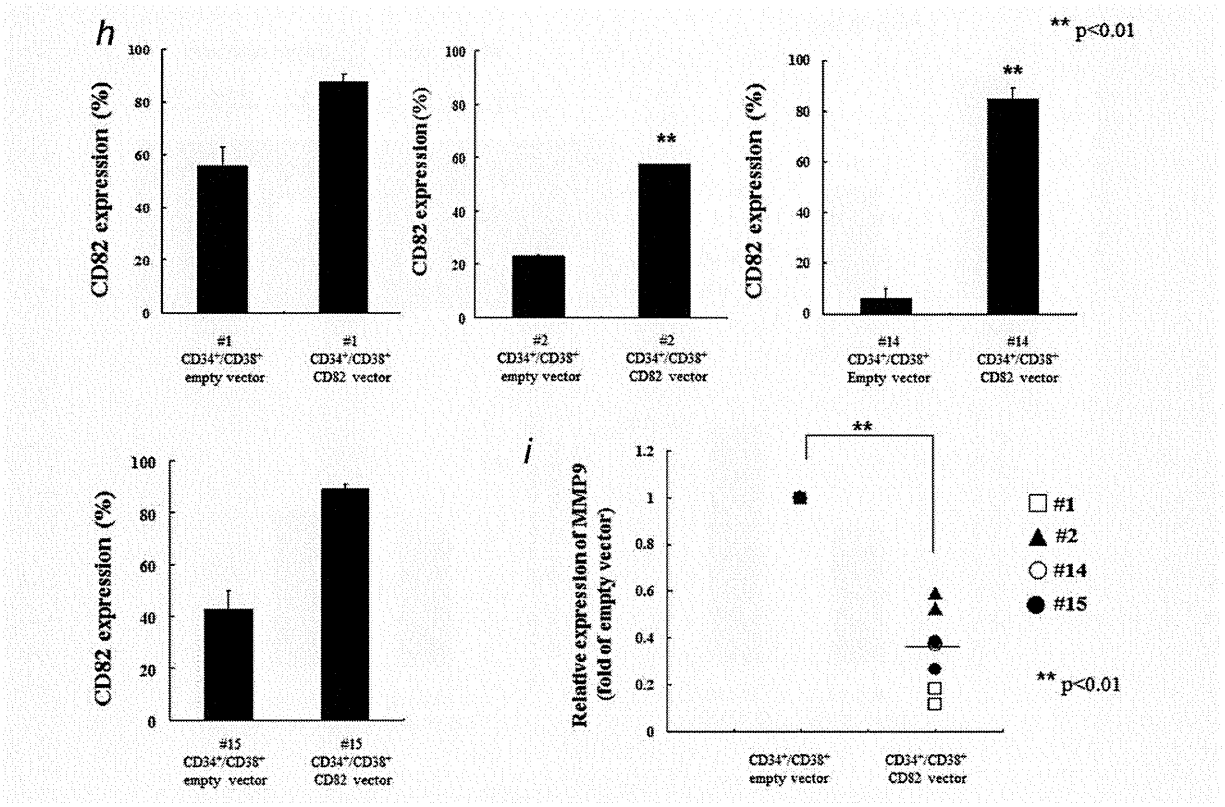

Figure 1. (Continued)

down-regulation of CD82 by an siRNA increased levels of MMP9 by nearly twofold in EOL-1R cells (Fig. 1*e*). On the other hand, levels of MMP2 were not affected by down-regulation of CD82 (Fig. 1*e*). Moreover, to explore the function of CD82 in freshly isolated $CD34^+/CD38^-$ AML cells, we genetically down-regulated CD82 in these cells. An shRNA targeting CD82 decreased expression of CD82 in four cells (case 1, from 85 ± 2% to 47 ± 3%; case 2, from 75 ± 1% to 13 ± 2%; case 6, from 47 ± 7% to 21 ± 3%, $p = 0.066$; case 14, from 43 ± 1% to 18 ± 1%, Fig. 1*f*). Real-time RT-PCR found that the levels of MMP9 were significantly increased after down-regulation of CD82 in $CD34^+/CD38^-$ AML cells ($n = 3$, cases 1, 2, and 6, $p < 0.05$, Fig. 1*g*). We next exposed $CD34^+/CD38^+$ AML cells to the CD82-expressing lentiviral particles, which increased levels of CD82 ($n = 4$, case 1; from 56 ± 7% to 88 ± 3%, case 2, from 23 ± 1% to 58 ± 1%; case 14; from 6 ± 4% to 85 ± 4%, case 15; from 43 ± 7% to 89 ± 2%, Fig. 1*h*). As expected, the levels of MMP9 were decreased by half in these cells (Fig. 1*i*).

The effects of CD82 on migration of $CD34^+/CD38^-$ AML cells

We next examined the function of CD82 in $CD34^+/CD38^-$ AML cells. When levels of CD82 were down-regulated in $CD34^+/CD38^-$ AML cells after lentiviral transduction of CD82 shRNA ($n = 4$. cases 1, 2, 6 and 14, Fig. 1*f*), their migration was significantly stimulated (Fig. 2*a*). Moreover, we enhanced expression of CD82 in $CD34^+/CD38^+$ AML cells by using CD82-expressing lentiviral particles ($n = 3$, cases 1, 14 and 15, Fig. 1*h*). Forced-expression of CD82 in $CD34^+/CD38^+$ AML cells dramatically increased number of cells adhered to the insert in parallel with a decrease in the number of migrated cells (Fig. 2*b*). Similarly, after down-regulation of CD82 in EOL-1R cells, adhesive cells decreased by approximately half (Fig. 2*c*). In parallel, population of EOL-1R cells migrated to the lower well increased by 10-fold after down-regulation of CD82 in these cells (Fig. 2*c*).

The effect of CD82 on colony forming ability of $CD34^+/CD38^-$ AML cells

We first examined whether CD82 regulated proliferation of $CD34^+/CD38^-$ AML cells (cases 1, 6, and 14) by using colony forming assay (Fig. 3*a*). Down-regulation of CD82 by an shRNA (from 59 to 27%) inhibited their colony forming ability by approximately 50% (Fig. 3*a*). Likewise, down-regulation of CD82 by an siRNA (from 96% to 48%) inhibited colony forming ability of $CD34^+$ EOL-1R cells which mimic LSCs by mean 50% (Fig. 3*b*). On the other hand, forced-expression of CD82 in $CD34^+/CD38^+$ AML cells (cases 1 and 14) by transduction of CD82-expressing lentiviral particles increased levels of CD82 from 18 to 89% and stimulated their colony forming ability by mean 1.7-fold (Fig. 3*c*).

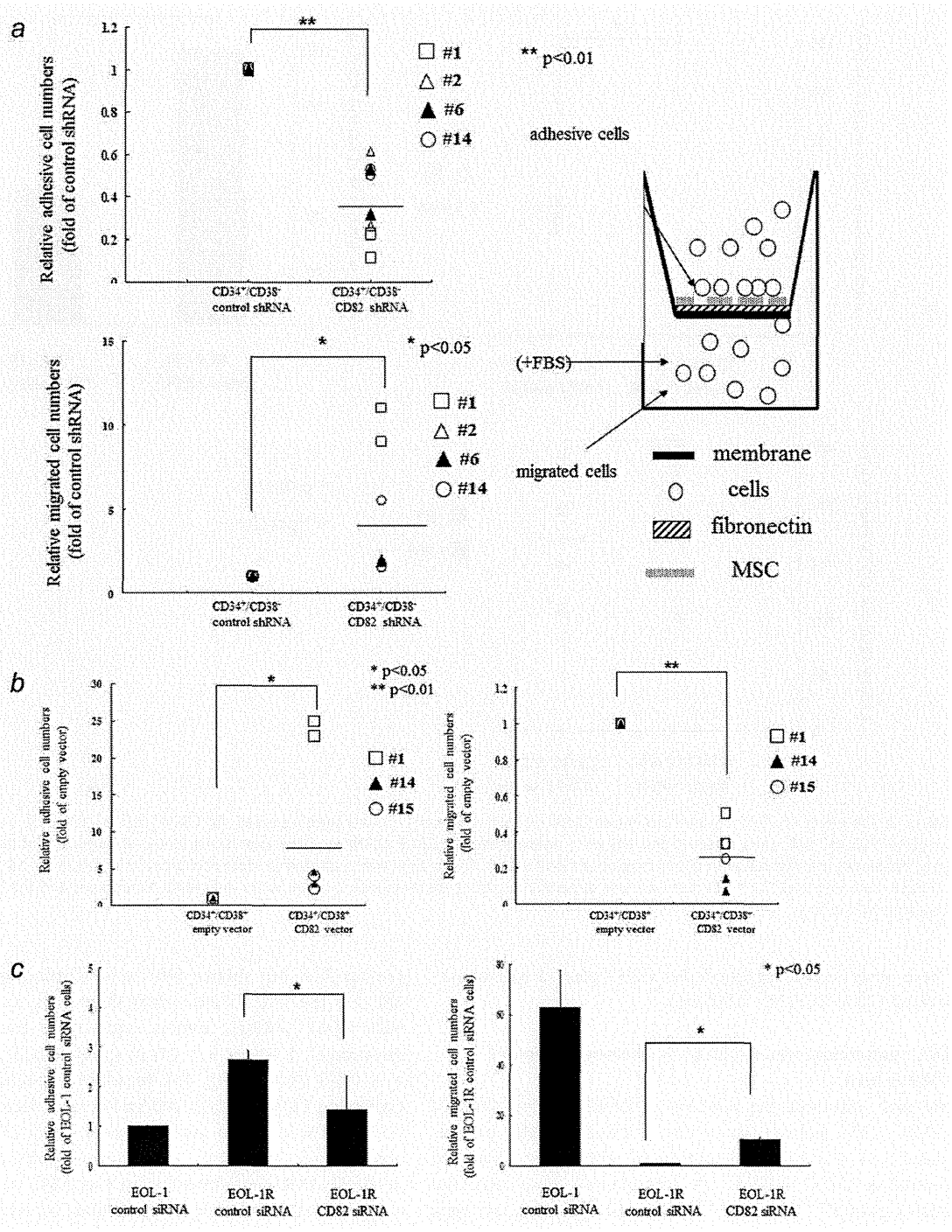

Figure 2. The effects of CD82 on migration of leukemia cells. Migration assays. (*a*) $CD34^+/CD38^-$ (cases 1, 2, 6, and 14) or (*b*) $CD34^+/CD38^+$ AML cells (cases 1, 14, and 15) transduced with CD82 shRNA or CD82-expressing lentiviral particle were seeded in the upper biocoat cell culture inserts. After 48 hr, the cells that had migrated through the filters were stained with 4'6-diamidino-2-phenylindole, and counted under a microscope. Each dot represents relative adhesion or migration cell numbers for an individual experiment and the mean is indicated by the line. (*c*) EOL-1 and EOL-1R cells transfected by either scrambled control or CD82 siRNA were seeded in the upper biocoat cell culture inserts. After 48 hr, the cells that had migrated through the filters were stained with 4'6-diamidino-2-phenylindole, and counted under a microscope. Results represent the mean ± SD of two experiments performed in triplicate cultures. $^{**}p < 0.01$; $^{*}p < 0.05$.

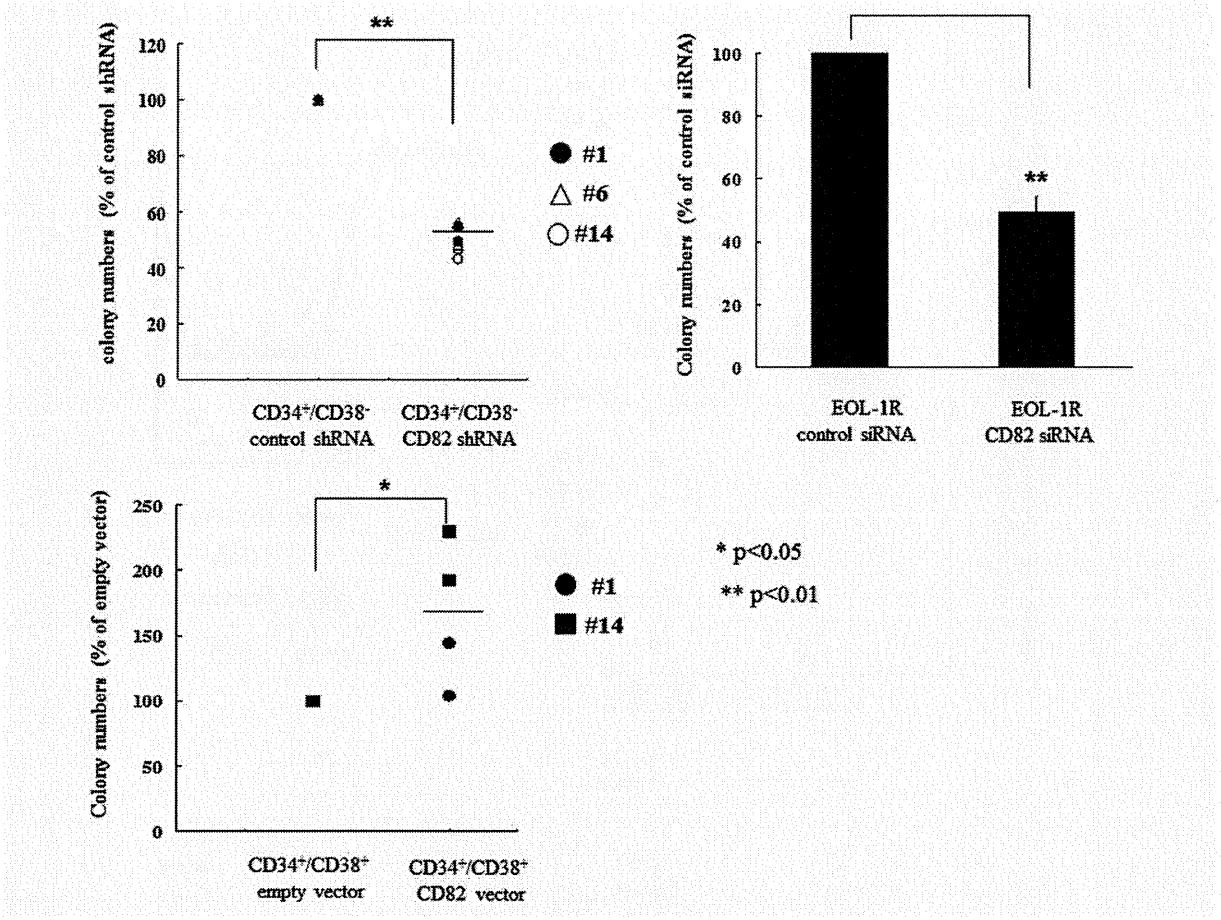

Figure 3. The effect of CD82 on proliferation of $CD34^+/CD38^-$ AML cells. Colony forming assay. (*a*) $CD34^+/CD38^-$ (cases 1, 6, and 14) or (*c*) $CD34^+/CD38^+$ AML cells (cases 1 and 14) were transduced with CD82 shRNA or CD82-expressing lentiviral particles. (*b*) EOL-1R cells were transiently transfected with either control or CD82 siRNA. These cells were cultured in methylcellulose medium. After 16 days, colonies were counted. Each dot represents % of colony number compared with control for an individual experiment and the mean is indicated by the line.

These observations suggested that CD82 plays a role in survival of $CD34^+/CD38^-$ AML cells.

AML engraftment was inhibited by down-regulation of CD82 *in vivo*

We next examined the function of CD82 *in vivo*. $CD34^+/CD38^-$ cells isolated from three different AML patients (cases 1, 6 and 14) were transduced with either scrambled control or CD82 shRNA. We transplanted these cells into NOD.Cg-*Rag1*^{tm1Mom} *Il2rg*^{tm1Wjl}/SzJ mice *via* the tail vein. Transplanted mice were sacrificed at 9 weeks after transplantation and analyzed the human engraftment in their spleens and BM by quantifying the population of positive cells for human CD45 and CD33 antigens (Figs. 4*a* and 4*b*). Transplantation of $CD34^+/CD38^-$ AML cells transduced by scrambled control shRNA resulted in the mean human engraftment either 14 ± 6% or 15 ± 5% in spleen and BM, respectively ($n = 8$, Fig. 4*a*). These cells expressed CD33antigen on their cell surface (4% in both spleen and BM) (Fig. 4*b*). On the other hand, when these cells were transduced with CD82 shRNA, human engraftment was significantly impaired (7 ± 4% or 6 ± 2% in spleen and BM, respectively, $p < 0.01$) ($n = 6$, Fig. 4*a*). In addition, population of cells expressing CD33 on their cell surface was decreased to either 0.1% or 1% in spleen and BM, respectively (Fig. 4*b*). These observations suggested that down-regulation of CD82 impaired AML engraftment as well as AML reconstitution in an immunodeficient mice. In addition, we assessed levels of CD82 and MMP9 in isolated $CD34^+/CD38^-$ AML cells ($n = 9$) by using single cell real-time RT-PCR (Fig. 4*c*). Inverse correlation was noted between levels of CD82 and MMP9 ($r = -0.58$, Fig. 4*c*). Moreover, we examined the levels of CD82 in transplanted human AML cells as well as localization of these cells in murine BM by immunohistochemistry (Figs. 4*d*–4*g*). Notably, human AML cells expressing CD82 were localized in endosteal region of BM at 9 weeks after

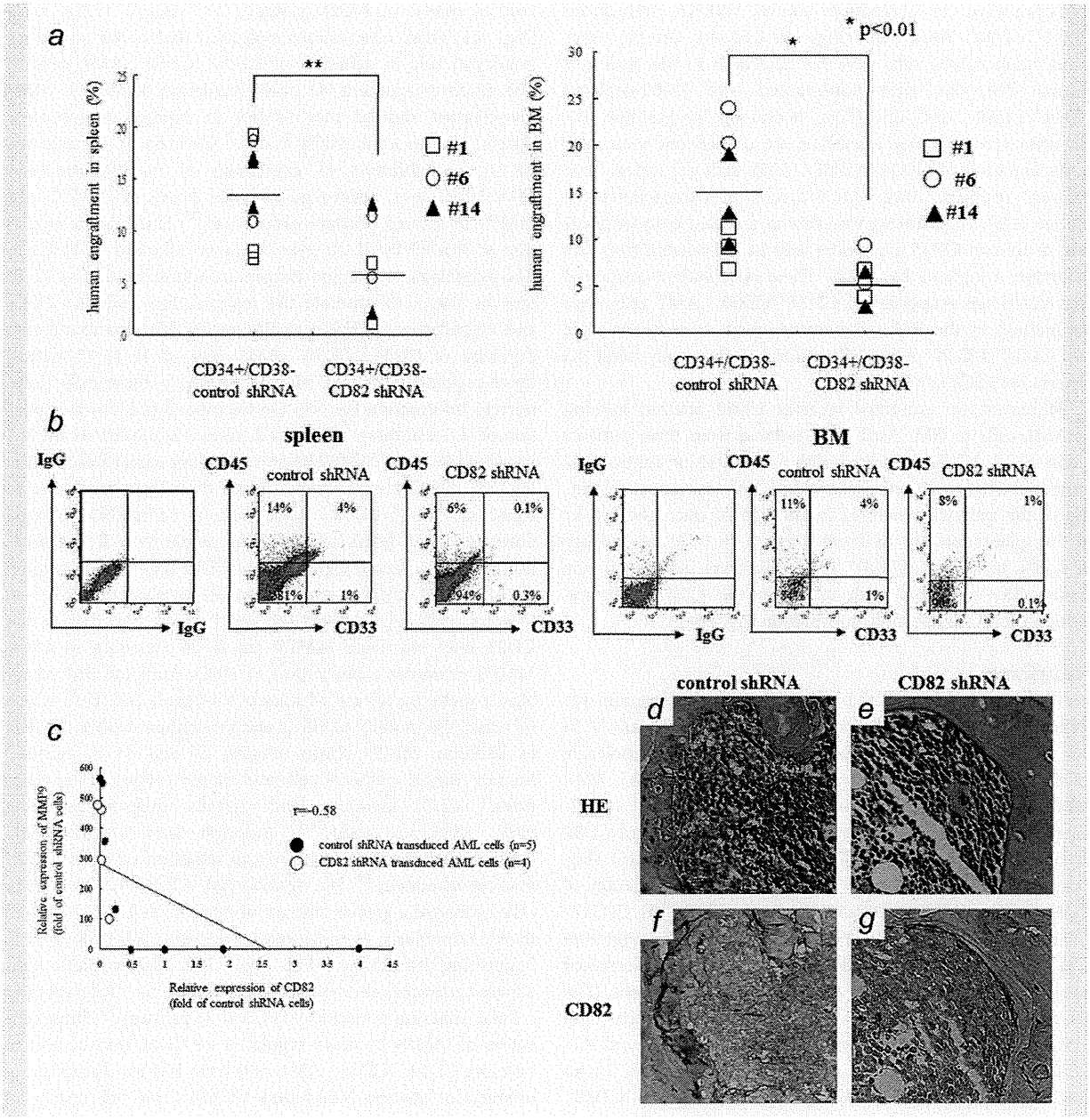

Figure 4. Down-regulation of CD82 impairs the AML engraftment. $CD34^+/CD38^-$ AML cells were isolated from three AML patients (cases 1, 6, and 14) and transduced with either scrambled control or CD82 shRNA. These cells were transplanted into NOD.Cg-*Rag1*^{tm1Mom} *Il2rg*^{tm1Wjl}/SzJ mice *via* the tail vein. At 9 weeks after transplantation, mice were euthanized and then spleen were removed. AML engraftment. (*a*) The percentages of human CD45 were analyzed to monitor the human engraftment in murine spleen and BM (scrambled control shRNA; $n = 8$, CD82 shRNA; $n = 6$) by using flow cytometry. Each dot represents CD45 expression for an individual experiment and the mean is indicated by the line. FACS. (*b*) Spleen and BM cells isolated from NOD.Cg-*Rag1*^{tm1Mom} *Il2rg*^{tm1Wjl}/SzJ mice received transplantation of $CD34^+/CD38^-$ AML cells (cases 1, 6, and 14) transduced with either CD82 shRNA or control shRNA were stained with anti-human CD45 and CD33 antibodies. Representative flow cytometric analyses of human CD45 and CD33 expression in murine spleen and BM cells are shown. Relationship between MMP9 and CD82. (*c*) A single $CD34^+/CD38^-$ AML cell was isolated from murine BMs by BD FACS AriaII. These cells were subjected to reverse transcription by AmpliSpeed slide cycler and the synthesized cDNA was subjected to real-time PCR to measure the levels of CD82 and MMP9. Results showed relative expression of MMP9 *versus* that of CD82. For demonstration of association, the Pearson's correlation coefficient test was applied. ●Scrambled control shRNA; $n = 5$, ○CD82 shRNA; $n = 4$. Immunohistochemistry. BMs were removed from mice, who were transplanted with either (*d*, *f*) scrambled control or (*e*, *g*) CD82 shRNA transduced $CD34^+/CD38^-$ AML cells. These BMs were stained with either (*d*, *e*) hematoxylin and eosin (HE) or (*f*, *g*) an anti-human CD82 antibody (CD82) and examined under light microscope.

transplantation of scrambled control shRNA transduced $CD34^+/CD38^-$ AML cells (Figs. 4*d* and 4*f*). On the other hand, human AML cells were not detectable in this region of murine BM, that were transplanted with CD82-depleted $CD34^+/CD38^-$ AML cells (Figs. 4*e* and 4*g*). To examine longer-term reconstituting capability, we carried out secondary transplantation of $CD34^+/CD38^-$ AML cells recovered from primary recipient mice. At 9 weeks post-transplantation, human AML engraftment was 18% as assessed by quantification of human CD45 expressing cells in PB isolated from the secondary recipients by FACS. These observations suggested that functional properties of $CD34^+/CD38^-$ AML cells were maintained in the BM microenvironment of recipient mice and $CD34^+/CD38^-$ AML cells utilized in this study fulfill the criteria for LSCs *in vivo*.

Moreover, we examined whether CD82 affected homing of AML cells to BM. AML cells isolated from three patients (cases 6, 14, 17) were treated with anti-CD82 or control IgG antibody. These cells were transplanted per mouse, and homing of the cells was analyzed in the BM of mice after 16 hr of transplantation. In the control group ($n = 6$), an average of 0.39% in human $CD34^+$ AML cells were detected in the mouse BM compared with 0.77% in the CD82 antibody-treated group (Supporting Information Fig. S6).

Discussion

Previous studies showed that the LSCs-niche interaction was important to maintain the stemness of leukemia cells.[15] In this study, iTRAQ technique identified adhesion molecule CD82 as an overexpressed protein in $CD34^+/CD38^-$ AML cells (Supporting Information Table S1). Additional experiments utilizing FACS confirmed aberrant expression of CD82 in freshly isolated $CD34^+/CD38^-$ AML cells ($n = 16$) (Fig. 1*a*). In addition, this study found that down-regulation of CD82 by an shRNA increased levels of MMP9 in $CD34^+/CD38^-$ AML cells (Fig. 1*g*) and stimulated their migration (Fig. 2*a*). Meanwhile, forced expression of CD82 decreased levels of MMP9 mRNA in $CD34^+/CD38^+$ AML cells (Fig. 1*i*) and enhanced adhesion of these cells to fibronectin and MSCs, a kind of artificial BM niche (Fig. 2*b*). Single cell RT-PCR also demonstrated that down-regulation of CD82 by an shRNA increased levels of MMP9 mRNA in $CD34^+/CD38^-$ AML cells, and reverse correlation was noted between levels of MMP9 and CD82 in $CD34^+/CD38^-$ AML cells (Fig. 4*c*). The levels of MMP9 mRNA in $CD34^+/CD38^-$ AML cells shown in Figures 1*g* and 4*c* were inconsistent, although the cells utilized in these studies were isolated from same populations. In these studies shown in Figure 4*c*, we used a single cell immediately after isolation from murine BM. On the other hand, cells used in these studies shown in Figure 1*g* were incubated for 7 days in full media to be transduced by shRNA. As a result, the levels of MMP9 mRNA in leukemia cells might be down-regulated in these cells. Notably, down-regulation of CD82 in $CD34^+/CD38^-$ AML cells ($n = 3$) by an shRNA impaired engraftment of these cells in the BM as well as spleen in NOD.Cg-*Rag1*^{tm1Mom} *Il2rg*^{tm1Wjl}/SzJ mice (Fig. 4*a*). These observations suggested that CD82 played an important role in adhesion of $CD34^+/CD38^-$ AML cells to BM microenvironment *via* down-regulation of MMP9. Other investigators showed that MMP9 in human mononuclear phagocytes was inhibited by IL-10.[32] Similarly, IL-10 activated the tissue inhibitors of expression of metalloproteinases (TIMP-1/2) and down-regulated the levels of MMP2 and MMP9 in human prostate cancer cells.[33] Thus, down-regulation of MMP9 by IL-10 may augment adhesion of HSCs to BM osteoblastic niche and exogenous administration of IL-10 may be useful to promote the repopulating ability of HSCs and engraftment of HSCs to BM niche. We also found that exposure of $CD34^+/CD38^-$ AML cells to IL-10 (5 ng/ml) down-regulated levels of MMP9 mRNA in these cells (Supporting Information Fig. S5). On the other hand, down-regulation of IL-10 in these cells ($n = 2$, cases 2 and 6) by an shRNA increased levels of MMP9 by twofold (Supporting Information Fig. S5). Further experiments found that down-regulation of CD82 in $CD34^+/CD38^-$ AML cells by an shRNA potently down-regulated levels of IL-10 (in preparation for publication). Notably, forced expression of CD82 down-regulated levels of MMP9 mRNA, resulting in inactivation of MMP9 in leukemia cells (Figs. 1*d* and 1*e*). We therefore hypothesize that CD82 may inactivate MMP9 *via* IL-10 signaling in LSCs. MMP9 promotes mobilization of HSCs from the BM osteoblastic niche by release of soluble Kit-ligand (sKitL),[34] which increases the motility of HSCs and progenitors within the BM. In addition, MMPs cleave integrin β4 and β1 in cultured human corneal epithelial cells and mouse epidermal keratinocytes.[35] CD82 associates with various integrins including α3β1, α4β1 and α6β1.[36,37] Amongst them integrin α4β1 (VLA4) plays an important role in adhesion of LSCs to BM microenvironment.[38] We found that $CD34^+/CD38^-$ AML cells expressed a greater amount of integrin α4β1 (VLA4) than their counterparts, as measured by real time RT-PCR ($n = 5$, Supporting Information Fig. S7*a*). The hematopoietic cells adhere to stromal endothelial cells through the VLA4/vascular cellular adhesion molecule-1 (VCAM-1) pathway.[39] Thus, activation of MMP9 by down-regulation of CD82 may be able to mobilize $CD34^+/CD38^-$ AML cells from BM *via* disruption of interaction between VLA4 and VCAM-1 on cell surface of stromal cells. Moreover, to assess if CD82 interacts with VLA4 molecules, we utilized an anti-integrin β1 (CD29) Ab (Beckman coulter, CA, 6603113) which blocks adhesion of leukemia cells to fibronectine. Forced-expression of CD82 stimulated an adhesion of $CD34^+/CD38^+$ AML cells (case 15) to the artificial niche, which was hampered when these cells were treated with an anti-integrin β1 Ab (Supporting Information Fig. S7*b*). Furthermore, we examined interaction between CD82 and integrin α4 by utilizing Immunoprecipitation assay and found that CD82 directly interacted with integrin α4 (Supporting Information Fig. S7*c*). These observations suggested that VLA4 interacted with CD82 and played a role in adhesion of these cells to the artificial niche.

We found that blockade of CD82 on cell surface of AML cells by an antibody stimulated BM homing of $CD34^+$ AML cells in these mice (Supporting Information Fig. S6). Similar to the present study, other investigates also showed that cord blood (CB) $CD34^+$ cells treated with stem cell factor enhanced expression of MMP2/MMP9 and increased BM homing of human CB $CD34^+$ cells in NOD/SCID mice.[40,41] Thus, blockade of CD82 may increase levels of MMP9, resulting in enhanced migration of AML cells into the BM. However, we hypothesize that these cells could not fully adhere to the BM microenvironment and survive to develop AML.

Interestingly, the CXCR4 antagonist AMD3100 effectively mobilized AML cells without inducing their proliferation.[42] Preclinical studies showed that treatment of leukemic mice with a chemotherapeutic agent in combination with AMD3100 resulted in decreased tumor burden and improved their overall survival compared with mice treated with a chemotherapeutic agent alone. These observations provided a proof-of-principle for directing therapy to the critical tethers that promote AML-niche interactions[42] and supported our hypothesis that inhibition of CD82 could mobilize LSCs from BM niche and sensitize these cells to chemotherapeutic agents. Further studies are clearly required to test our hypothesis *in vivo*.

Another idea to sensitize LSCs to chemotherapeutic agents related to stimulation of cell-cycling of dormant LSCs. Recent studies showed that $CD34^+/CD38^-$ AML cells were induced to enter the cell cycle by treatment with G-CSF *in vivo*. G-CSF significantly enhanced apoptosis of $CD34^+/CD38^-$ AML cells mediated by cell cycle-dependent chemotherapeutic agents and eliminated $CD34^+/CD38^-$ AML cells from mice.[43] The additional experiments found that down-regulation of CD82 was not able to stimulate cell cycling of $CD34^+/CD38^-$ AML cells (cases 1 and 6) and EOL-1R cells (Supporting Information Fig. S3), suggesting that CD82 was not involved in the maintenance of dormancy in these cells.

CD82 inhibited the receptor tyrosine kinase human mesenchymal-epithelial transition factor (c-Met) activity,[44] which promoted proliferation and migration of cancer cells.[45,46] c-Met was shown to mediate G-CSF-induced mobilization of hematopoietic progenitor cells (HPCs) *via* reactive oxygen species (ROS) signaling.[47] Aberrant expression of CD82 in $CD34^+/CD38^-$ AML cells may inactivate c-Met and cause engraftment of these cells to BM niche. We found that levels of CD82 in $CD34^+$ hematopoietic stem/progenitor cells isolated from healthy volunteers ($n = 6$) were lower than those in $CD34^+/CD38^-$ AML cells (35% *vs.* 59%, $p = 0.02$, Supporting Information Fig. S4). Importantly, down-regulation of CD82 in $CD34^+$ hematopoietic stem/progenitor cells by an shRNA did not significantly inhibit their colony forming ability (Supporting Information Fig. S4).

CD82 expression was strongly correlated with the tumor suppressor gene p53.[48] On the other hand, other studies showed that levels of CD82 did not correlate with the expression of p53 in human hepatocellular carcinoma.[49] We also examined the correlation between CD82 and p53 mRNA levels in $CD34^+/CD38^-$ AML cells ($n = 6$) and their $CD34^+/CD38^-$ counterparts by utilizing real-time RT-PCR and found that the correlation coefficient was 0.54 (figure not shown). Thus, we think that expression of CD82 is not related with p53 in $CD34^+/CD38^-$ AML cells.

Overexpressed CD82 in AML cells may render these cells to adhere to BM niche and regulate maintenance of leukemia stem cells within BM niche. On the other hand, down-regulation of CD82 in AML cells may stimulate circulating of these cells from BM niche to PB.

Taken together, our data suggested that CD82 negatively regulated MMP9 and played an important role in $CD34^+/CD38^-$ AML cells to adhere to BM microenvironment. In addition, CD82 was involved in survival of $CD34^+/CD38^-$ AML cells. CD82 might be an attractive molecular target to eradicate LSCs in AML patients. Further studies are warranted to evaluate the function of CD82 in LSCs *in vivo*.

Acknowledgements

This work was supported in part by The Kochi University President's Discretionary Grant (to T.I.), Setsuro Fujii Memorial, The Osaka Foundation for Promotion of Fundamental Medical Research (to T.I.) and Certificate of Kochi Shin-kin/Anshin-tomo-no-kai Prize (to C.N.). C.N. is grateful for a JSPS Research Fellowship for Young Scientists from the Japan Society for the Promotion of Science.

References

1. Bonnet D, Dick JE. Human acute myeloid leukemia is organized as a hierarchy that originates from a primitive hematopoietic cell. *Nat Med* 1997;3:730–7.
2. Lapidot T, Sirard C, Vormoor J, et al. A cell initiating human acute myeloid leukaemia after transplantation into SCID mice. *Nature* 1994;367:645–8.
3. Blair A, Sutherland HJ. Primitive acute myeloid leukemia cells with long-term proliferative ability in vitro and in vivo lack surface expression of c-kit (CD117). *Exp Hematol* 2000;28:660–71.
4. Blair A, Hogge DE, Sutherland HJ. Most acute myeloid leukemia progenitor cells with long-term proliferative ability in vitro and in vivo have the phenotype CD34(+)/CD71(-)/HLA-DR-. *Blood* 1998;92:4325–35.
5. Clarke MF, Dick JE, Dirks PB, et al. Cancer stem cells-perspectives on current status and future directions: AACR Workshop on cancer stem cells. *Cancer Res* 2006;66:9339–44.
6. Ishikawa F, Yoshida S, Saito Y, et al. Chemotherapy-resistant human AML stem cells home to and engraft within the bone-marrow endosteal region. *Nat Biotechnol* 2007;25:1315–21.
7. Taussig DC, Miraki-Moud F, Anjos-Afonso F, et al. Anti-CD38 antibody-mediated clearance of human repopulating cells masks the heterogeneity of leukemia-initiating cells. *Blood* 2008;112:568–75.
8. Sarry JE, Murphy K, Perry R, et al. Human acute myelogenous leukemia stem cells are rare and heterogeneous when assayed in NOD/SCID/IL2Rγc-deficient mice. *J Clin Invest* 2011;121:384–95.
9. Schofield R. The trelationship between the spleen colony foming cell and the haematopoietic stem cell. *Blood Cell* 1978;4:7–25.
10. Nilsson SK, Haylock DN, Johnston HM, et al. Hyaluronan is synthesized by primitive hematopoietic cells, participates in their lodgment at the endosteum following transplantation, and is involved in the regulation of their proliferation

and differentiation in vitro. *Blood* 2003;101: 856–62.
11. Zhang J, Niu C, Ye L, et al. Identification of the haematopoietic stem cell niche and control of the niche size. *Nature* 2003;425:836–41.
12. Calvi LM, Adams GB, Weibrecht KW, et al. Osteoblastic cells regulate the haematopoietic stem cell niche. *Nature* 2003;425:841–6.
13. Tavor S, Petit I, Porozov S, et al. CXCR4 regulates migration and development of human acute myelogenous leukemia stem cells in transplanted NOD/SCID mice. *Cancer Res* 2004; 64:2817–24.
14. Jin L, Hope KJ, Zhai Q, et al. Targeting of CD44 eradicates human acute myeloid leukemic stem cells. *Nat Med* 2006;12:1167–74.
15. Avigdor A, Goichberg P, Shivtiel S, et al. CD44 and hyaluronic acid cooperate with SDF-1 in the trafficking of human CD34+ stem/progenitor cells to bone marrow. *Blood* 2004;103:2981–9.
16. Dong JT, Lamb PW, Rinker-Schaeffer CW, et al. KAI1, a metastasis suppressor gene for prostate cancer on human chromosome 11p11.2. *Science* 1995;268:884–86.
17. Ruseva Z, Geiger PX, Hutzler P, et al. Tumor suppressor KAI1 affects integrin alphavbeta3-mediated ovarian cancer cell adhesion, motility, and proliferation. *Exp Cell Res* 2009;315:1759–71.
18. Jee BK, Park KM, Surendran S, et al. KAI1/CD82 suppresses tumor invasion by MMP9 inactivation via TIMP1 up-regulation in the H1299 human lung carcinoma cell line. *Biochem Biophys Res* 2006;342:655–61.
19. Popov C, Radic T, Haasters F, et al. Integrins α2β1 and α11β1 regulate the survival of mesenchymal stem cells on collagen I. *Cell Death Dis* 2011;2:e186.
20. Ikezoe T, Yang J, Nishioka C, et al. Inhibition of signal transducer and activator of transcription 5 by the inhibitor of janus kinases stimulates dormant human leukemia CD34(+) /CD38(-) cells and sensitizes them to antileukemia agents. *Int J Cancer* 2011;128:2317–25.
21. Nishioka C, Ikezoe T, Yang J, et al. Long-term exposure of leukemia cells to multi-targeted tyrosine kinase inhibitor induces activations of AKT, ERK and STAT5 signaling via epigenetic silencing of the PTEN gene. *Leukemia* 2010;24: 1631–40.
22. Werb Z, Vu TH, Rinkenberger JL, et al. Matrix-degrading proteases and angiogenesis during development and tumor formation. *APMIS* 1999; 107:11–18.
23. Serada S, Fujimoto M, Ogata A, et al. iTRAQ-based proteomic identification of leucine-rich alpha-2 glycoprotein as a novel inflammatory biomarker in autoimmune diseases. *Ann Rheum Dis* 2010;69:770–4.
24. Ikezoe T, Tanosaki S, Krug U, et al. Insulin-like growth factor binding protein-3 antagonizes the effects of retinoids in myeloid leukemia cells. *Blood* 2004;104:237–42.
25. Ikezoe T, Takeuchi T, Yang J, et al. Analysis of Aurora B kinase in non-Hodgkin lymphoma. *Lab Invest* 2009;89:1364–73.
26. Pearson T, Shultz LD, Miller D, et al. Non-obese diabetic-recombination activating gene-1 (NOD-Rag1 null) interleukin (IL)-2 receptor common gamma chain (IL2r gamma null) null mice: a radioresistant model for human lymphohaematopoietic engraftment. *Clin Exp Immunol* 2008;154:270–84.
27. Unwin RD, Pierce A, Watson RB, et al. Quantitative proteomic analysis using isobaric protein tags enables rapid comparison of changes in transcript and protein levels in transformed cells. *Mol Cell Proteomics* 2005;4:924–35.
28. Ran D, Schubert M, Pietsch L, et al. Aldehyde dehydrogenase activity among primary leukemia cells is associated with stem cell features and correlates with adverse clinical outcomes. *Exp Hematol* 2009;37:1423–34.
29. Gal H, Amariglio N, Trakhtenbrot L, et al. Gene expression profiles of AML derived stem cells; similarity to hematopoietic stem cells. *Leukemia* 2006;20:2147–54.
30. Muranyi AL, Dedhar S, Hogge DE. Targeting integrin linked kinase and FMS-like tyrosine kinase-3 is cytotoxic to acute myeloid leukemia stem cells but spares normal progenitors. *Leuk Res* 2010;34:1358–65.
31. Xie W, Wang X, Du W, et al. Detection of molecular targets on the surface of CD34+ CD38$^-$ bone marrow cells in myelodysplastic syndromes. *Cytometry A.* 2010;77:840–8.
32. Lacraz S, Nicod LP, Chicheportiche R, et al. IL-10 inhibits metalloproteinase and stimulates TIMP-1 production in human mononuclear phagocytes. *J Clin Invest* 1995;96:2304–10.
33. Stearns ME, Fudge K, Garcia F, et al. IL-10 inhibition of human prostate PC-3 ML cell metastases in SCID mice: IL-10 stimulation of TIMP-1 and inhibition of MMP-2/MMP-9 expression. *Invasion Metastasis* 1997;17:62–74.
34. Heissig B, Hattori K, Dias S, et al. Recruitment of stem and progenitor cells from the bone marrow niche requires MMP-9 mediated release of kit-ligand. *Cell* 2002;109:625–37.
35. Pal-Ghosh S, Blanco T, Tadvalkar G, et al. MMP9 cleavage of the β4 integrin ectodomain leads to recurrent epithelial erosions in mice. *J Cell Sci* 2011;124:2666–75.
36. Iwata S, Kobayashi H, Miyake-Nishijima R, et al. Distinctive signaling pathways through CD82 and beta1 integrins in human T cells. *Eur J Immunol* 2002;32:1328–37.
37. Berditchevski F, Kraeft SK, Chen LB, et al. Transmembrane-4 superfamily proteins CD81 (TAPA-1), CD82, CD63, and CD53 specifically associated with integrin alpha 4 beta 1 (CD49d/ CD29). *J Immunol* 1996;157:2039–47.
38. Matsunaga T, Takemoto N, Sato T, et al. Interaction between leukemic-cell VLA-4 and stromal fibronectin is a decisive factor for minimal residual disease of acute myelogenous leukemia. *Nat Med* 2003;9:1158–65.
39. Papayannopoulou T, Priestley GV, Nakamoto B. Anti-VLA4/VCAM-1-induced mobilization requires cooperative signaling through the kit/ mkit ligand pathway. *Blood* 1998;91:2231–9.
40. Byk T, Kahn J, Kollet O, et al. Cycling G1 CD34+/CD38+ cells potentiate the motility and engraftment of quiescent G0 CD34+/CD38$^-$/low severe combined immunodeficiency repopulating cells. *Stem Cells* 2005;23:561–74.
41. Zheng Y, Sun A, Han ZC. Stem cell factor improves SCID-repopulating activity of human umbilical cord blood-derived hematopoietic stem/ progenitor cells in xenotransplanted NOD/SCID mouse model. *Bone Marrow Transplant* 2005;35: 137–42.
42. Nervi B, Ramirez P, Rettig MP, et al. Chemosensitization of acute myeloid leukemia (AML) following mobilization by the CXCR4 antagonist AMD3100. *Blood* 2009;113:6206–14.
43. Saito Y, Uchida N, Tanaka S, et al. Induction of cell cycle entry eliminates human leukemia stem cells in a mouse model of AML. *Nat Biotechnol* 2010;28:275–80.
44. He B, Liu L, Cook GA, et al. Tetraspanin CD82 attenuates cellular morphogenesis through down-regulating integrin alpha6-mediated cell adhesion. *J Biol Chem* 2005;280:3346–54.
45. Christensen JG, Burrows J, Salgia R. c-Met as a target for human cancer and characterization of inhibitors for therapeutic intervention. *Cancer Lett* 2005;225:1–26.
46. Danilkovitch-Miagkova A, Zbar B. Dysregulation of Met receptor tyrosine kinase activity in invasive tumors. *J Clin Invest* 2002; 109:863–7.
47. Tesio M, Golan K, Corso S, et al. Enhanced c-Met activity promotes G-CSF-induced mobilization of hematopoietic progenitor cells via ROS signaling. *Blood* 2011;117:419–28.
48. Marreiros A, Dudgeon K, Dao V, et al. KAI1 promoter activity is dependent on p53, junB and AP2: evidence for a possible mechanism underlying loss of KAI1 expression in cancer cells. *Oncogene* 2005;24:637–49.
49. Jackson P, Ow K, Yardley G, et al. Expression and clinical significance of p53, JunB and KAI1/ CD82 in human hepatocellular carcinoma. *Hepatobiliary Pancreat Dis Int* 2009;8:389–96.

IJC
International Journal of Cancer

Plasma membrane proteomics identifies bone marrow stromal antigen 2 as a potential therapeutic target in endometrial cancer

Takuhei Yokoyama[1,2], Takayuki Enomoto[1], Satoshi Serada[2], Akiko Morimoto[1,2], Shinya Matsuzaki[1,2], Yutaka Ueda[1], Kiyoshi Yoshino[1], Masami Fujita[1], Satoru Kyo[3], Kota Iwahori[2], Minoru Fujimoto[2], Tadashi Kimura[1] and Tetsuji Naka[2]

[1] Department of Obstetrics and Gynecology, Osaka University Graduate School of Medicine, Osaka, Japan
[2] Laboratory for Immune Signal, National Institute of Biomedical Innovation, Osaka, Japan
[3] Department of Obstetrics and Gynecology, Kanazawa University Graduate School of Medicine, Kanazawa, Japan

This report utilizes a novel proteomic method for discovering potential therapeutic targets in endometrial cancer. We used a biotinylation-based approach for cell-surface protein enrichment combined with isobaric tags for relative and absolute quantitation (iTRAQ) technology using nano liquid chromatography–tandem mass spectrometry analysis to identify specifically overexpressed proteins in endometrial cancer cells compared with normal endometrial cells. We identified a total of 272 proteins, including 11 plasma membrane proteins, whose expression increased more than twofold in at least four of seven endometrial cancer cell lines compared with a normal endometrial cell line. Overexpression of bone marrow stromal antigen 2 (BST2) was detected and the observation was supported by immunohistochemical analysis using clinical samples. The expression of BST2 was more characteristic of 118 endometrial cancer tissues compared with 59 normal endometrial tissues ($p < 0.0001$). The therapeutic effect of an anti-BST2 antibody was studied both *in vitro* and *in vivo*. An anti-BST2 monoclonal antibody showed *in vitro* cytotoxicity in BST2-positive endometrial cancer cells *via* antibody-dependent cell-mediated cytotoxicity and complement-dependent cytotoxicity. In an *in vivo* xenograft model, anti-BST2 antibody treatment significantly inhibited tumor growth of BST2-positive endometrial cancer cells in an NK cell-dependent manner. The anti-BST2 antibody had a potent antitumor effect against endometrial cancer both *in vitro* and *in vivo*, indicating a strong potential for clinical use of anti-BST2 antibody for endometrial cancer treatment. The combination of biotinylation-based enrichment of cell-surface proteins and iTRAQ analysis should be a useful screening method for future discovery of potential therapeutic targets.

Key words: endometrial cancer, molecular target, plasma membrane, iTRAQ, BST2

Abbreviations: ADCC: antibody-dependent cell-mediated cytotoxicity; BST2: bone marrow stromal antigen 2; calcein-AM: calcein-acetoxymethyl ester; CDC: complement-dependent cytotoxicity; E/T ratio: effector to target ratio; FACS: fluorescence activated cell sorting; iTRAQ: isobaric tags for relative and absolute quantitation; LC: liquid chromatography; MS/MS: tandem mass spectrometry; NOD: nonobese diabetic; qRT-PCR: quantitative reverse transcription-PCR; SCID: severe combined immunodeficient; SCX: strong cation exchange; siRNA: small interfering RNA.
Additional Supporting Information may be found in the online version of this article.

Grant sponsors: Grant-in-Aid for Scientific Research from the Japanese Ministry of Education, Science, Culture and Sports, Grant-in-Aid from the Ministry of Health, Labour and Welfare of Japan
DOI: 10.1002/ijc.27679
History: Received 5 Mar 2012; Accepted 30 May 2012; Online 22 Jun 2012

Correspondence to: Tetsuji Naka, Laboratory for Immune Signal, National Institute of Biomedical Innovation, 7-6-8 Saitoasagi, Ibaraki City, Osaka 567-0085, Japan, Tel.: +81-72-641-9843, Fax: +81-72-641-9837, E-mail: tnaka@nibio.go.jp

Anticancer monoclonal antibodies are a growing family of novel agents applied in the treatment regimens for hematopoietic and solid tumors. Antibody-based therapeutic agents against CD20 or Her2 have been successfully clinically developed and have significant therapeutic effects.[1,2] Tumor-associated antigens which are easily accessible from the tumor neovasculature are particularly attractive for intravenously-administered antibody-based therapeutic agents. During the last decade, several new technologies for high-throughput screening have identified many potential therapeutic targets. Thus far, no single approach or combination of methods has emerged as the preferred paradigm. It is clear that new tools and strategies are needed so that tumor-associated antigens can be screened efficiently.

Proteomic methods can now be tailored to search directly for targetable cell-surface proteins that distinguish cancer cells from normal cells. The complexity and concentration of individual proteins in the sample are crucial when performing proteomic analyses because abundant proteins, such as cytoskeletal proteins, may hinder the detection of low abundance proteins, such as plasma membrane proteins.[3] One way to enrich the potentially accessible cell-surface proteins is by whole cell protein tagging followed by affinity purification. A method for enrichment of such cell-surface proteins

What's new?
In this study, we have used a biotinylation-based approach for cell-surface protein enrichment combined with iTRAQ technology to identify and quantify membrane proteins which might represent potential therapeutic targets of endometrial cancer. A monoclonal antibody targeting BST2, one of the proteins identified in the iTRAQ analysis, have a potent antitumor effect against endometrial cancer both *in vitro* and *in vivo*, indicating a strong potential for clinical use of anti-BST2 antibody for endometrial cancer treatment.

via their biotinylation and affinity purification has been reported.[4,5] In most cases, concentrated cell-surface proteins are separated by SDS-PAGE and the enzymatically digested peptides are analyzed by mass spectrometry, while highly accurate quantitative data cannot be obtained by using this method. To acquire more quantitative information, stable isotope labeling using amino acids in cell culture (SILAC) based quantitative proteomics has been used, with high quantitative accuracy; however, the SILAC approach has the limitation that only a maximum of three samples can run in any single analysis.[6,7] Compared with SILAC, the more recently developed isobaric tags for relative and absolute quantitation (iTRAQ) technology has a distinct advantage regarding sample number handling capability in a single analysis, because iTRAQ can compare up to eight samples simultaneously.[7,8]

Endometrial cancer is the most common malignant tumor of the female genital tract. Its incidence varies among regions; it is overall the fourth most common malignancy in North America.[9] In general, the prognosis of these patients is excellent as the majority present with early-stage disease that is confined to the uterus at the time of diagnosis, which is followed by simple hysterectomy, leading to a 5-year survival rate of 84%.[9] Unfortunately, those women who present with recurrent or advanced-stage disease have a much poorer prognosis, with a median survival of less than a year.[10] To date, combination chemotherapy of cisplatin, doxorubicin, and paclitaxel has demonstrated the greatest efficacy.[10–12] However, these cytotoxic agents are associated with intolerable side effects and infrequent sustainable remission.[11,12] Thus, new and more effective targeted therapies for endometrial cancer are urgently needed. However, thus far the search for agents effective in the treatment of either recurrent or advanced endometrial cancer has been disappointing.[12]

Aiming for the identification of surface-accessible tumor antigens best suitable for antibody-based therapeutic intervention, it is important to analyze plasma membrane proteins known to be involved in endometrial cancer. For this purpose, we have utilized a novel proteomic technology by combining biotinylation-based approach for cell membrane enrichment and iTRAQ technology using nano liquid chromatography–tandem mass spectrometry (LC-MS/MS) analysis. In this study, one normal endometrial cell line (EM-E6/E7/TERT cells, immortalized normal endometrial cells) and seven endometrial cancer cell lines were used as a comparative model for studying the plasma membrane proteins related to endometrial cancer. Among 272 proteins identified by iTRAQ analysis, bone marrow stromal antigen 2 (BST2) was investigated in more detail. By immunohistochemical analysis using actual clinical specimens, we found that the expression level of BST2 was significantly higher in endometrial cancer tissues compared with normal endometrial tissues. An anti-BST2 antibody showed potent antibody-dependent cell-mediated cytotoxicity (ADCC) and complement-dependent cytotoxicity (CDC) against BST2-positive endometrial cancer cells *in vitro*. In an *in vivo* xenograft model, anti-BST2 antibody treatment significantly inhibited tumor growth.

Taken together, our strategy of screening cell-surface tumor-specific antigens might be useful for identifying new therapeutic targets.

Material and Methods

Cell lines and cultures

We previously established an immortalized normal endometrial cell line (EM-E6/E7/TERT cells).[13,14] Nine human endometrial cancer cell lines (HEC-1, HEC-1A, HEC-6, HEC-88nu, HEC-108, HEC-116, HEC-251, SNG-II, and SNG-M cells) were obtained from the Japanese Collection of Research Bioresources (JCRB, Osaka, Japan), where they were tested and authenticated on June 30, 2011. The method used for testing was multiplexed PCR amplification of eight short tandem repeat loci (TH01, D5S818, D13S317, D7S820, D16S539, CSF1PO, vWA, and TPOX) and amelogenin was performed using the PowerPlex^{TM}16 System (Promega, Madison, WI). PCR-amplified fragments were analyzed with an ABI PRISM 310 Genetic Analyzer (Applied Biosystems, Foster City, CA). Then the fragments were typed based on allelic ladders. EM-E6/E7/TERT cells were maintained in a 1:1 mixture of DMEM and Ham's F12 medium (Wako Pure Chemical Industries, Osaka, Japan) supplemented with 10% FBS (HyClone Laboratories, Logan, UT) and 1% penicillin-streptomycin (Nacalai Tesque, Kyoto, Japan) at 37°C under a humidified atmosphere of 5% CO_2. HEC-1, HEC-1A, HEC-6, HEC-88nu, HEC-108, HEC-116, and HEC-251 cells were maintained and propagated in DMEM (Wako Pure Chemical Industries) supplemented with 10% FBS and 1% penicillin-streptomycin. SNG-II and SNG-M cells were maintained in Ham's F12 (Invitrogen, Carlsbad, CA) with 10% FBS and 1% penicillin-streptomycin.

Biotinylation of bovine serum albumin (BSA)

BSA (30 μM) was biotinylated with a 100-fold molar excess of sulfosuccinimidyl 2-(biotinamido)-ethyl-1,3-dithiopropionate

(sulfo-NHS-SS-biotin; Pierce, Rockford, IL) and desalted as described previously.[15]

Capture of cell-surface proteins

To isolate cell-surface proteins, the normal endometrial cell line (EM-E6/E7/TERT cells) and seven endometrial cancer cell lines (HEC-1, HEC-1A, HEC-6, HEC-108, HEC-116, HEC-251, and SNG-II cells) were grown to approaching confluency (up to 90%) in three 15 cm dishes. Cells were washed three times with prewarmed PBS and then the cell-surface proteins were biotinylated for 15 min at room temperature with 15 ml of 500 μM sulfo-NHS-SS-biotin solution dissolved in PBS. The residual biotinylation reagent was quenched with 5 mM lysine for 5 min at room temperature. After biotinylation, the cells were washed with PBS twice, harvested by scraping, and collected by centrifugation (1,500 rpm, 4°C, 5 min). Detailed methods of extraction and purification of biotinylated cell-surface proteins are described in the Supporting Information Materials and Methods section.

iTRAQ labeling

Trypsin-digested peptides were dissolved in 5 μl of 9.8 M urea and 20 μl of 1M TEAB. Samples were labeled with the iTRAQ reagent according to the manufacturer's protocol (Applied Biosystems). EM-E6/E7/TERT cells were labeled with iTRAQ reagent 113, HEC-1 cells with 114, HEC-1A cells with 115, HEC-6 cells with 116, HEC-108 cells with 117, HEC-116 cells with 118, HEC-251 cells with 119, and SNG-II cells with 121. The labeled peptide samples were then pooled and desalted with Sep-Pak Light C18 Cartridges (Waters, Manchester, UK) and peptides were dried in a centrifugal concentrator (Micro Vac MV-100, Tomy, Tokyo, Japan) before strong cation exchange (SCX) fractionation.

SCX fractionation

In order to remove excess unreacted iTRAQ reagent and to simplify the complexity of the peptide mixture, the labeled peptide mixtures were purified and fractionated using SCX column (SCX, PolySulfoethyl A column, 2.1 × 150 mm, 5 μm, 300 Å) on an Agilent 1200 HPLC system. Detailed information is provided in the Supporting Information Materials and Methods section.

Mass spectrometric analysis

Nano LC-MS/MS analyses were performed on an LTQ-Orbitrap XL (Thermo Fisher Scientific, Waltham, MA) equipped with a nano-ESI source and coupled to a Paradigm MG4 pump (Michrom Bioresources, Auburn, CA) and autosampler (HTC PAL, CTC Analytics, Zwingen, Switzerland). Detailed information is provided in the Supporting Information Materials and Methods section.

iTRAQ data analysis

Protein identification and quantification for iTRAQ analysis was carried out using Proteome Discoverer software (v. 1.1) (Thermo Fisher Scientific) against Swiss Prot human protein database (SwissProt_2011_11, 533,049 entries). Taxonomy was set to *Homo sapiens* (20,326 entries) or mammalian (65,656 entries). Search parameters for peptide and MS/MS mass tolerance were 10 ppm and 0.8 Da, respectively, with allowance for two missed cleavages made from the trypsin digest. Carbamidomethylation (Cys) and iTRAQ8plex (Lys, N-terminal) were specified as static modifications, whereas CAMthiopropanoyl (Lys, N-terminal), iTRAQ8plex (Tyr), and oxidation (Met) were specified as variable modifications in the database search. The false discovery rate of 1% was calculated by Proteome Discoverer based on a search against a corresponding randomized database. Relative protein abundances were calculated using the ratio of iTRAQ reporter ion in the MS/MS scan. For subcellular localization, all the proteins identified in this analysis were analyzed using the UniprotKB (available at: http://www.uniprot.org/) and Ingenuity Pathway Analysis software (Ingenuity Systems, Redwood City, CA).

Quantitative reverse transcription-PCR (qRT-PCR) analysis

To confirm the altered expression of BST2 in endometrial cancer, the normal endometrial cell line (EM-E6/E7/TERT cells) and nine endometrial cancer cell lines (HEC-1, HEC-1A, HEC-6, HEC-88nu, HEC-108, HEC-116, HEC-251, SNG-II, and SNG-M cells) were subjected to qRT-PCR. Total RNA was extracted using an RNeasy Mini Kit (Qiagen, Valencia, CA) and cDNAs were synthesized with a QuantiTect Reverse Transcription Kit (Qiagen), all according to the manufacturers' instructions. qRT-PCR was performed using SYBR Premix Ex taq (Takara Bio, Shiga, Japan) and an ABI 7900HT real-time PCR instrument (Applied Biosystems). β-Actin was used as a housekeeping gene for normalization of quantitative real-time PCR analysis. The primer sequences and the expected sizes of PCR products were as follows: BST2, forward primer 5′-GGAGGAGCTTGAGGGAGAG-3′ and reverse primer 5′-CTCAGTCGCTCCACCTCTG-3′, 75 bp; β-actin, forward primer 5′-AGCCTCGCCTTTGCCGA-3′ and reverse primer 5′-CTGGTGCCTGGGGCG-3′, 174 bp. Relative quantitation of gene expression was performed using the standard curve method as outlined by Applied Biosystems. Experimental conditions were tested in triplicate and three independent experiments were performed.

Fluorescence activated cell sorting (FACS) analysis

Cells were washed twice in PBS (Nacalai Tesque) and detached with 0.02% EDTA solution (Nacalai Tesque). Cells were washed twice with cold FACS buffer (PBS supplemented with 1% FBS and 0.1% sodium azide) and then incubated with mouse anti-human BST2 antibody (Biolegend, San Diego, CA) at a 1:100 dilution and labeled with Alexa Fluor 488-labeled donkey anti-mouse IgG antibody (Invitrogen). Stained cells were analyzed using a FACS Canto cytometer (Becton Dickinson, Mountain View, CA) and the results were analyzed using FlowJo software (Tree Star, Stanford, CA).